The Structure and Evolution of a Continental Winter Cyclone. Part I: Frontal Structure and the Occlusion Process

JONATHAN E. MARTIN

Department of Atmospheric and Oceanic Sciences, University of Wisconsin—Madison, Madison, Wisconsin

(Manuscript received 5 September 1996, in final form 9 June 1997)

ABSTRACT

The frontal structure and occlusion process in a cyclone of moderate intensity that affected the central United States in January 1995 is examined. The deep warm-frontal zone associated with this cyclone had a lateral extension to the southwest of the sea level pressure minimum that, although characterized by cold-air advection near the surface, had many of the characteristics of a warm front aloft. In fact, this feature had a structure similar to the so-called bent-back fronts previously documented only in association with explosively deepening maritime cyclones.

The development of a warm-occluded structure was investigated with the aid of a numerical simulation of the event performed using the University of Wisconsin—Nonhydrostatic Modeling System. The development of the warm-occluded structure was asynchronous in the vertical; occurring first at midtropospheric levels and later near the surface, in contrast to the classical occlusion process. Near the surface, the warm-occluded front was formed as the warm front was overtaken by the frontogenetically inactive portion of the historical cold-frontal zone. At midtropospheric levels, the warm occluded structure formed as a result of the cold-frontal zone approaching, and subsequently ascending, the warm-frontal zone in accord with a component of the classical occlusion mechanism.

The observed asynchronous evolution of the occluded structure is proposed to result from the vertical variation in vortex strength associated with the upper-level potential vorticity (PV) anomaly that controls the cyclogenesis. It is suggested that the occlusion process begins aloft, where the associated vortex strength is greatest, and gradually penetrates downward toward the surface during the cyclone life cycle. Additionally, a characteristic ''treble clef'' shape to the upper-level PV anomaly is shown to be a sufficient condition for asserting the presence of a warm-occluded structure in the underlying troposphere.

1. Introduction

The structure and evolution of winter cyclones in the central United States has recently come under renewed scrutiny. The considerable baroclinicity that characterizes the continental winter, coupled with the steady progression of synoptic-scale baroclinic disturbances in the westerlies and their interaction with the unique geography of the region leads to the development of an array of cyclonic disturbances in the central United States that exhibit a variety of frontal structures. Winter cyclones that affect this region also vary in intensity from the occasional explosive deepener to the much more common modest surface cyclone in which sometimes steady, but often weak, development occurs for a period of 1–2 days.

Various aspects of the rare explosively deepening continental cyclones such as their frontal structure (Mass and Schultz 1993), the dynamics of the cyclogenesis (Hakim et al. 1995), the occurrence of and forcing mechanisms for mesoscale gravity waves (Uccellini and Koch 1987; Schneider 1990; Powers and Reed 1993; Pokrandt et al. 1996) as well as the forcing of mesoscale bands of heavy snow (Marwitz and Toth 1993) have been investigated recently. Additionally, the structure of occluded cyclones and the nature of the occlusion process has been considered in the context of explosive continental development (Schultz and Mass 1993).

The more common, but less intense, winter cyclones that characterize this region have been investigated as well. The influence of the Rocky Mountains on the frontal structure and precipitation distribution of some of these storms (Martin et al. 1995; Wang et al. 1995; Locatelli et al. 1995; Castle et al. 1996) has led to the development of a new conceptual model for a particular set of these cyclones (Hobbs et al. 1996). Along similar lines, the inverted trough in the sea level pressure field (Keshishian et al. 1994) is a structural artifact of the interaction of mobile baroclinic disturbances with the orography of the northern Great Plains.

It is not uncommon for members of this set of modest cyclones to be associated with copious amounts of snowfall while experiencing little or no systematic sur-

Corresponding author address: Dr. Jonathan E. Martin, Dept. of Atmospheric and Oceanic Sciences, University of Wisconsin—Madison, 1225 West Dayton St., Madison, WI 53706.
E-mail: jon@meteor.wisc.edu

face development. Various mechanisms have been identified as factors in the development of such large snowfalls including frontogenesis in the presence of conditional symmetric instability (CSI) (Moore and Blakely 1988), favorable jet streak interactions (Shea and Pryzbylinski 1995), isentropic lift (Shea and Pryzbylinski 1993; Funk et al. 1995), as well as melting-induced frontal circulations (Rauber et al. 1994). Despite the insights into the mesoscale forcing of heavy snow provided by these case studies, none have investigated the synoptic evolution and frontal structure of the associated modest surface cyclone.

This series of papers will help fill this gap in our knowledge of winter cyclones in the central United States by presenting a detailed, observational/modeling study of such a modest continental cyclone that affected this region on 19–20 January 1995. The storm was fairly weak in terms of its sea level pressure minimum (which throughout its life cycle was never less than 997 hPa). Despite this fact, it was attended by an 1100-km-long, narrow band of snowfall greater than 25 cm that was forced by the dynamics and kinematics of the 3D airflow associated first with a warm front and then with an occluded front. The bent-back extension to the warm front above the planetary boundary layer is one of the ways in which the frontal structure of this storm resembled the ''fractured front'' model of Shapiro and Keyser (1990). This structure played an important role in both the production and distribution of precipitation during this event and contributed to the development of a warm-occluded (i.e., warm-type occlusion) structure.

In the present paper, routine synoptic observations at the surface and upper levels, wind profiler data, and a successful numerical simulation of this storm performed using the University of Wisconsin—Nonhydrostatic Modeling System (UW-NMS) are employed to examine the evolution of the frontal structure associated with this cyclone as well as the nature of the occlusion process. In Part II (Martin 1998), the dynamical forcing that produced the heavy snowband is investigated through use of a finer-scale simulation of this case using the UW-NMS.

Section 2 of the current paper will present an observational synoptic-scale analysis of the cyclone from 0000 UTC 19 January 1995 through 0000 UTC 20 January 1995. In section 3 a description of the numerical forecast model is given along with a discussion of the accuracy of the simulation. In sections 4 and 5 the model gridded data are used to further elucidate the frontal structure of this cyclone paying particular attention to the occlusion process and the development of the warm-occluded structure. Model trajectories, as well as thermodynamic surfaces, will be used to demonstrate that a component of the classical occlusion mechanism actually operated at midlevels in this cyclone. In section 6 comparison is made of results from this case to those of prior work on occluded structures. It is also suggested that the asynchronous development of the warm-occluded structure is a function of the large-scale environment and dynamics of the cyclogenesis. A tropopause potential vorticity structure that is a signature of some warm-occluded cyclones is identified. Final comments and conclusions are offered in section 7.

2. Observations of the synoptic evolution of the cyclone

a. 0000 UTC 19 January 1995

At 0000 UTC 19 January 1995, a surface low pressure center, with a minimum central pressure of 1003 hPa, was located in southcentral Arkansas (Fig. 1a). A surface cold front extended from eastern Louisiana into the western Gulf of Mexico and was marked by strong westerly flow behind it. The surface warm front had been the trailing cold front of a decaying system located along the southwestern shore of Hudson Bay before being incorporated into the developing low center in Arkansas. As evidenced by the high temperature and dewpoint values in Mississippi, a narrow tongue of high-θ_e surface air was advected toward the developing low center by strong southerly winds. Snowfall, which had begun at 2100 UTC 18 January in northeastern Oklahoma had become more widespread (it was snowing from McAllister, Oklahoma, to Columbia, Missouri) and Springfield, Missouri, reported heavy snow—the first of 13 consecutive hours of heavy snow at that station. The wind shift and temperature drop in northeast Texas at this time provided convincing evidence of a secondary frontal structure to the west and southwest of the surface low center. We shall refer to this secondary feature as the bent-back front based upon its structural similarity to frontal features, observed by Shapiro and Keyser (1990), that appear to be extensions of the warm-frontal zone to the southwest of the surface depression. A description of the evolution of this feature is beyond the scope of this paper and may be different, in the present case, from the evolution of such structures in maritime cyclones.

The 850-hPa geopotential height and temperature analysis (Fig. 1b) at this time also suggests the presence of this bent-back front. The 850-hPa potential temperature θ gradient over gulf coastal Texas is clearly the vertical extension of the primary surface cold front. The greater than 90° wind shift between Longview, Texas (GGG), and Fort Worth, Texas (DFW), and accompanying temperature gradient indicates the presence of a separate baroclinic zone there. This zone is the vertical extension of the bent-back front identified at the surface. Note how the bent-back baroclinic zone is a lateral extension of the northern edge of the intense warm frontal baroclinic zone that extends northeastward to the Great Lakes at this time.

The thermal structure was equally intriguing at 700 hPa (Fig. 1c). The primary cold-frontal baroclinic zone was clearly separate from a secondary region of cold-air advection in northeast Texas. Note the intense hor-

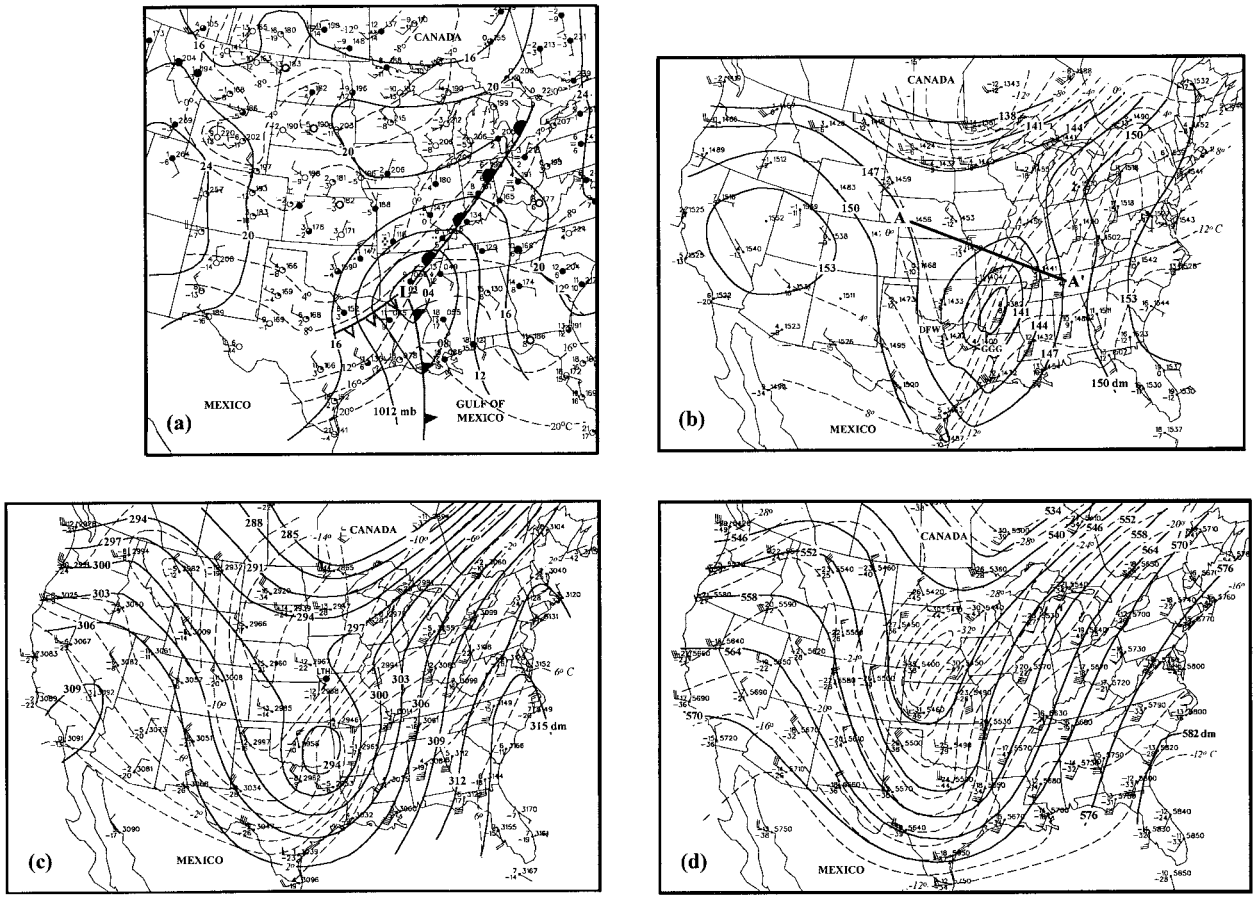

FIG. 1. (a) Sea level pressure analysis at 0000 UTC 19 January 1995. Solid lines are isobars (hPa) labeled and contoured every 4 hPa. Dashed lines are isotherms (°C) labeled and contoured every 4°C. Conventional frontal symbols indicate positions of surface fronts with open cold-frontal symbol depicting the bent-back front. For each surface station the following data are shown: temperature (°C, to the upper left of the station symbol), dewpoint (°C, to the lower left of the station symbol), sea level pressure [labeled in tenths of hectopascals, dropping the hundreds digit(s)], wind direction and speed, skycover, and present weather. Sky cover is shown using the following symbols: open circle—clear, one-quarter shaded circle—scattered clouds, one-half shaded circle—broken clouds, three-quarters shaded circle—mostly cloudy, fully shaded circle—overcast. Wind speeds are indicated by a circle around a circle—calm, half barb—$<$2.5 m s^{-1}, short barb—2.5 m s^{-1}, long barb—5 m s^{-1}, flag—25 m s^{-1}. Conventional present weather symbols are used with intensity of precipitation indicated by number of precipitation symbols at a station. (b) The 850-hPa analysis at 0000 UTC 19 January 1995. Solid lines are geopotential height (dam) labeled and contoured every 3 dam. Dashed lines are isotherms (°C) labeled and contoured every 2°C. For each station the following data are shown: temperature (°C, to the upper left of the station symbol), dewpoint (°C, to the lower left of the station symbol), geopotential height (m, to the upper right of the station symbol). Wind speed and direction are indicated as in Fig. 1a. A cross section along line *AA′* is shown in Fig. 2. Longview, Texas (GGG), and Fort Worth, Texas (DFW), are shown. (c) The 700-hPa analysis for 0000 UTC 19 January 1995. Analyzed as in Fig. 1b. Location of Lathrop, Missouri (LTH), is indicated. (d) The 500-hPa analysis for 0000 UTC 19 January 1995. Analyzed as in Fig. 1b except geopotential height (solid lines) are contoured every 6 dam.

izontal deformation along the warm frontal baroclinic zone from northern Illinois to northeastern Oklahoma where a region of warm-air advection is juxtaposed with a region of cold-air advection along the Missouri–Kansas border. This thermal and kinematic structure is characteristic of a developing warm front. It is clear that a portion of the warm-frontal baroclinic zone at this level extends to the southwest of the point of intersection of the primary cold frontal baroclinic zone with the warm-frontal baroclinic zone. This structure is reminiscent of the observed bent-back frontal structure described by Nieman and Shapiro (1993, see their Figs. 7 and 8) in their analysis of the ERICA IOP 4 explosively deepening maritime cyclone.

At 500 hPa (Fig. 1d) a deep longwave trough was centered over central Oklahoma and north-central Texas with a region of sharp curvature over northeastern Texas and Arkansas. A secondary shortwave was located over the Colorado–Nebraska–Kansas border and was associated with a developing upper-level front. This fact was made manifest in the development of a pool of very cold air at this level over central Nebraska. The development of this cold pool enhanced the 500-hPa thermal gradient over Kansas and Nebraska, thus adding to the

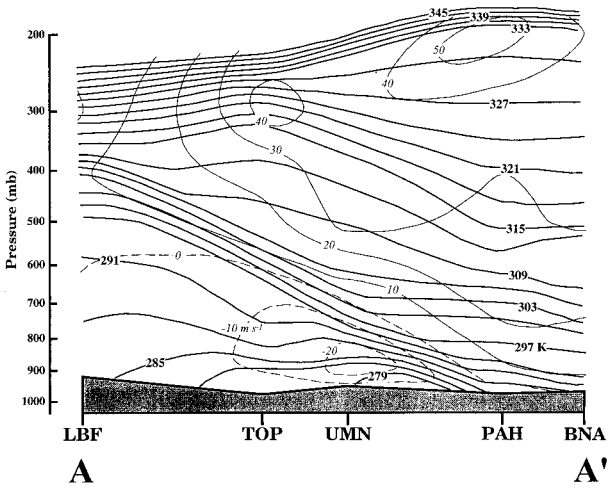

FIG. 2. A vertical cross section through the warm front, along line AA' in Fig. 1b, from North Platte, Nebraska (LBF), to Topeka, Kansas (TOP), to Monett, Missouri (UMN), to Paducah, Kentucky (PAH), to Nashville, Tennessee (BNA), at 0000 UTC 19 January 1995. Thick solid lines are contours of potential temperature θ (K) contoured every 3 K. Thin dashed (solid) lines are isotachs (m s^{-1}, contoured every 10 m s^{-1}) perpendicular to AA' directed out of (into) the page.

depth of the warm-frontal baroclinic zone observed at that time. The depth of this frontal zone is particularly evident in the cross section of potential temperature shown in Fig. 2.

b. 1200 UTC 19 January 1995

Between 0000 and 1200 UTC 19 January, the surface low deepened to 998 hPa and moved northeastward to a position southeast of St. Louis, Missouri (Fig. 3a). By this time, a well-developed squall line was situated along the primary surface cold front while a burgeoning band of heavy snow paralleled the warm front and the bent-back front from the lower peninsula of Michigan to the Missouri–Arkansas–Oklahoma border. The surface cyclone began to acquire an asymmetry in the sea level pressure distribution about this time as the pressure gradient was much larger north and west of the warm front and the bent-back front than to the east.

The equivalently modest development (as measured by geopotential height change) at 850 hPa deformed the isotherms at that level as shown in Fig. 3b. An intense low-level jet associated with the developing warm front advected a pocket of cool air ($T < -4$°C) from eastern Kansas into southeastern Arkansas. Warm-air advection at this level occurred from the Great Lakes to northwestern Arkansas exactly where the snowband existed at this time.

At 700 hPa, where distinct baroclinic zones had existed at 0000 UTC, the continued modest development led to further deformation of the isotherm pattern there (Fig. 3c). This thermal pattern is reminiscent of the ''frontal fracture'' phase of the T-bone conceptual model for explosive extratropical marine cyclones introduced by Shapiro and Keyser (1990). In this case, the warm-frontal baroclinic zone extended from the Great Lakes to northwestern Arkansas. East of this baroclinic zone, especially in southeastern Missouri, there was a fracture in the baroclinic structure of the cyclone. The main cold-frontal baroclinic zone extended from its intersection with the warm-frontal zone in central Illinois southwestward to New Orleans, Louisiana. We shall refer to the point of intersection of these two baroclinic zones as the *peak of the warm sector*. Intense frontogenesis (to be shown in Part II), a result of strong deformation superimposed upon the large horizontal temperature gradient, characterized the warm-frontal zone along its entire length. Not surprisingly, the snowband was located parallel to this active frontal feature.

Even more dramatic evidence of the similarity in structure of this cyclone to the T-bone conceptual structure is offered in the 700-hPa θ_e analysis (Fig. 4). The very sharp cold-frontal θ_e gradient stretched from the central Gulf of Mexico to north-central Illinois. In eastern Missouri and Arkansas there was a considerably weaker θ_e gradient with a completely different orientation (this is the frontal fracture region). It was bordered by the sharp warm-frontal θ_e gradient that ran from central Wisconsin to northwestern Arkansas. In addition, a tongue of high-θ_e air was just east of the cold front. This air was rapidly transported northward to the peak of the warm sector where it was forced to ascend the warm front. As a result, heavy snow fell along the Mississippi River in Iowa and northeastern Missouri around this time.

At 500 hPa (Fig. 3d) the upper-level front and its associated short-wave trough were located over central Oklahoma and continued to strengthen. Trough merger was about to occur between the initial wave that had spawned the surface cyclone (which was, at this time, located over southeast Missouri) and the invading upper-level front/short-wave system. The baroclinic zone extending from southern Iowa to the upper peninsula of Michigan was characterized by frontogenetical horizontal confluence at this time. The squall line was aligned along the leading edge of 500-hPa cold-air advection as described by Hobbs et al. (1990) and Locatelli et al. (1995). In contrast to their cases, the upper baroclinic zone in this case was the vertical extension of a bona fide surface cold front.

Although a hint of the characteristics of the bent-back front can be obtained by inspection of the several isobaric charts, illustrative vertical cross sections through the feature at 1200 UTC 19 January are given in Fig. 5. This cross section is taken along a line that lies to the southwest of the surface low at 1200 UTC and cuts the baroclinic zone along the bent-back front. In the potential temperature cross section (Fig. 5a), a shallow, well-defined frontal structure between Paducah, Kentucky (PAH), and Monett, Missouri (UMN), is evident. The winds veer with height (Fig. 5b) through the zone indicating that warm air advection occurs along it. This

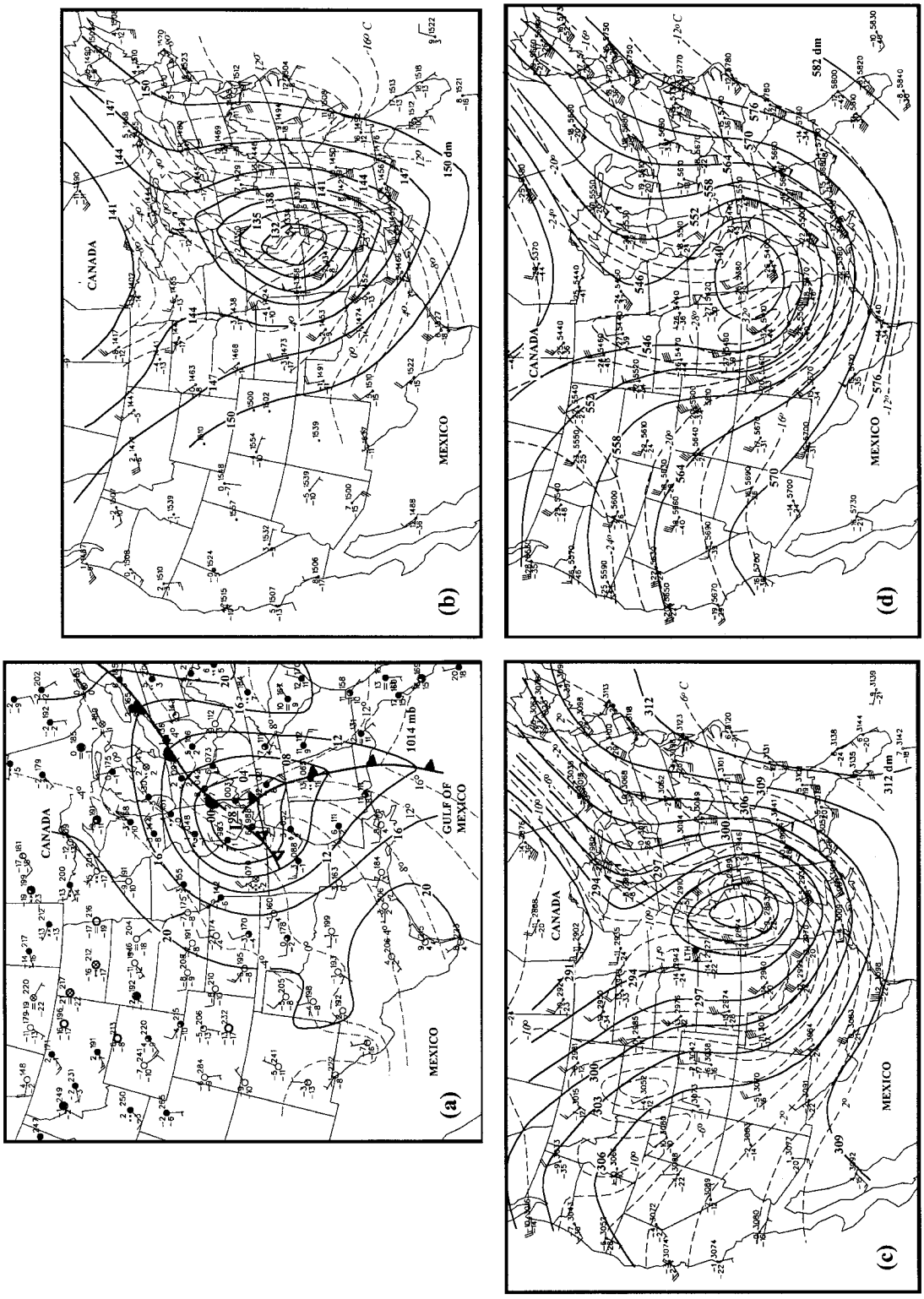

FIG. 3. (a) As in Fig. 1a except for 1200 UTC 19 January 1995. (b) As in Fig. 1b except for 1200 UTC 19 January 1995. (c) As in Fig. 1c except for 1200 UTC 19 January 1995. (d) As in Fig. 1d except for 1200 UTC 19 January 1995.

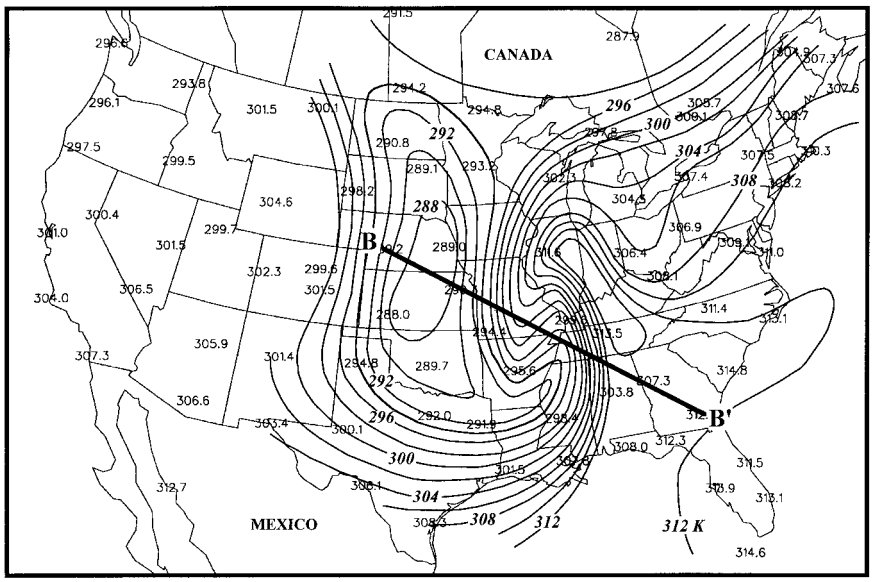

FIG. 4. Analysis of 700-hPa equivalent potential temperature θ_e at 1200 UTC 19 January 1995. Solid lines are moist isentropes (K) labeled and contoured every 2 K. A cross section along *BB′* is shown in Fig. 5.

can be verified by consideration of the isobaric geostrophic temperature advection inferred in Figs. 3b and 3c. This evidence suggests that the bent-back frontal zone, although characterized by cold-air advection at the surface, was actually behaving like a warm front through most of the lower troposphere at this time.

Additional evidence suggesting the same conclusion is a time series of profiler winds at Lathrop, Missouri (Fig. 6). This time series extends from 0000 UTC 19 January [at which time Lathrop was located on the cold edge of the warm frontal baroclinic zone at 700 hPa (see Fig. 1c)] to 1100 UTC 19 January [at which time Lathrop was in the cold air west of the warm-frontal baroclinic zone at 700 hPa (see Fig. 3c)]. Notice the layer of veering winds that is located at 700 hPa (~3000 m) at 0000 UTC. This layer steadily rises at the station with time indicating that a continuous zone of warm-air advection must have moved *southeastward* with time. Such a southeastward moving zone of warm-air advection in the Northern Hemisphere is consistent with the presence of a warm front to the southwest of the geopotential depression.

Figure 5b shows a cross section of equivalent potential temperature at 1200 UTC along the same line as Fig. 5a. The frontal zone is clearly delineated and is marked by a sharp θ_e contrast. An isolated region of potential instability was located over PAH. The nearly vertical orientation of the θ_e isopleths in the lowest 200 hPa of the frontal zone strongly suggests that the equivalent potential vorticity (EPV) was near or even less than zero. The implications of such a circumstance, along with the midlevel convective instability, on the production of heavy snow are discussed in Part II.

Between 1200 and 1800 UTC the surface cyclone center moved slightly northwestward. By 1800 UTC, the 998-hPa surface low pressure center was still located east of St. Louis, Missouri (Fig. 7). The bent-back front extended southwestward behind the surface low into northeastern Arkansas. The band of moderate to heavy snow persisted from central Missouri to the Wisconsin–Iowa border.

c. 0000 UTC 20 January 1995

The sea level pressure analysis for 0000 UTC 20 January is shown in Fig. 8a. By this time, surface redevelopment near the peak of the original warm sector had spawned a secondary surface low over south-central Ohio. The main surface cold front extended southward from the new surface low toward central Florida. A fairly vigorous, continuous line of convective precipitation had redeveloped along the cold front by this time in response to the flow of warm, moist, high-θ_e boundary layer air from over the Gulf Stream toward the surface cold front. By this time a surface warm-occluded front had developed as evidenced by the ridge in the surface isotherms that extended from western Ohio to western Kentucky. The surface warm occlusion had incorporated the weak surface bent-back front. Snowfall associated with the warm and occluded fronts stretched from northcentral Michigan to southeastern Missouri at this time.

At 850 hPa (Fig. 8b) a well-defined cold-frontal baroclinic zone was evident over the eastern United States. The warm-frontal zone extended from central Illinois toward James Bay, Ontario, and a ridge of maximum θ extended from northeastern Illinois to southeastern Mis-

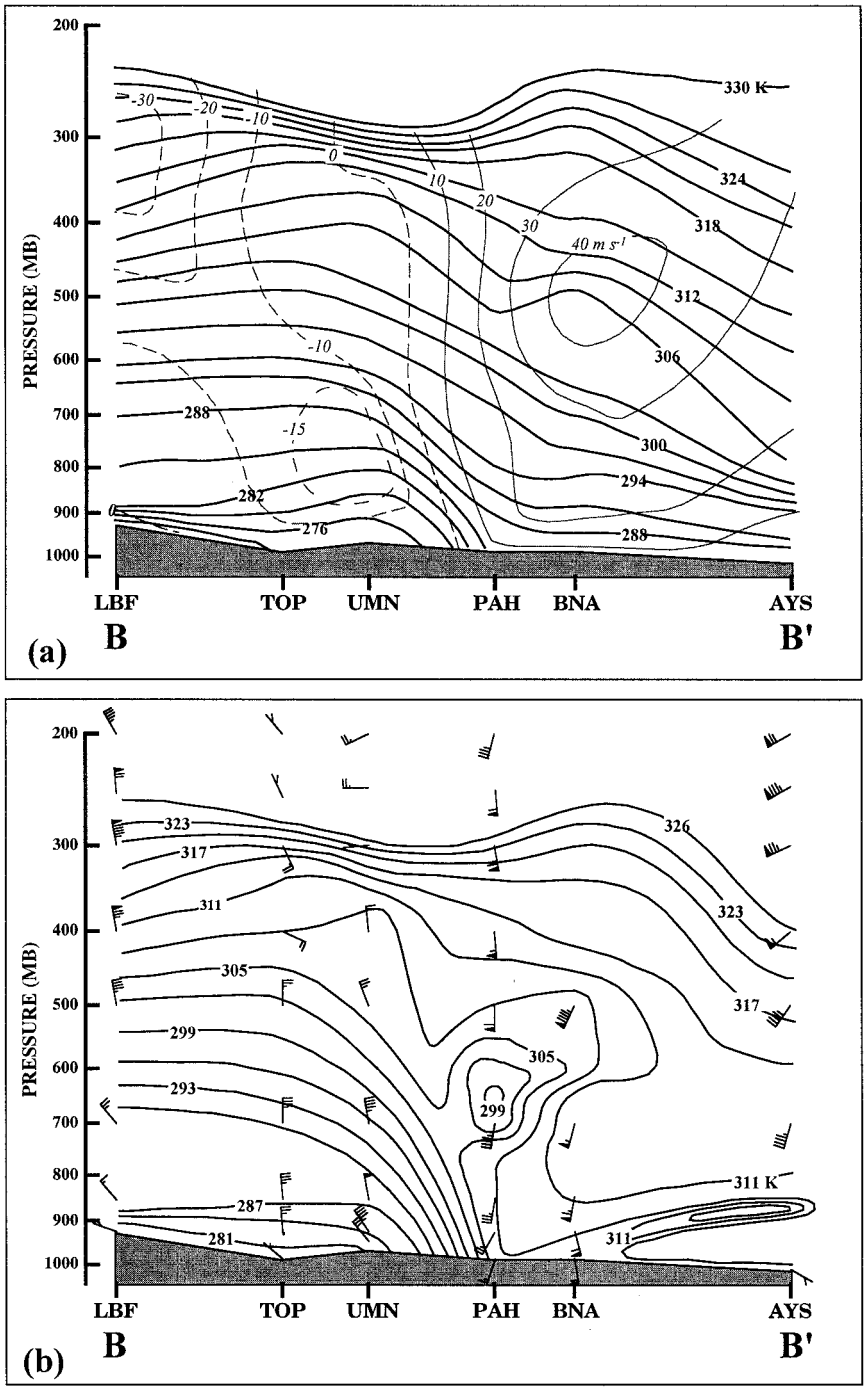

FIG. 5. (a) Vertical cross section, along *BB′* in Fig. 4, from North Platte, Nebraska (LBF), to Topeka, Kansas (TOP), to Monett, Missouri (UMN), to Paducah, Kentucky (PAH), to Nashville, Tennessee (BNA), to Waycross, Georgia (AYS), at 1200 UTC 19 January 1995. Thick solid lines are contours of potential temperature θ contoured every 3 K. Thin dashed (solid) lines are isotachs (m s^{-1}, contoured every 10 m s^{-1} except for the -15 m s^{-1} isotach) perpendicular to *BB′* directed out of (into) the page. (b) As for Fig. 5a except solid lines are contours of equivalent potential temperature θ_e contoured every 3 K. Wind barbs analyzed as in Fig. 1a.

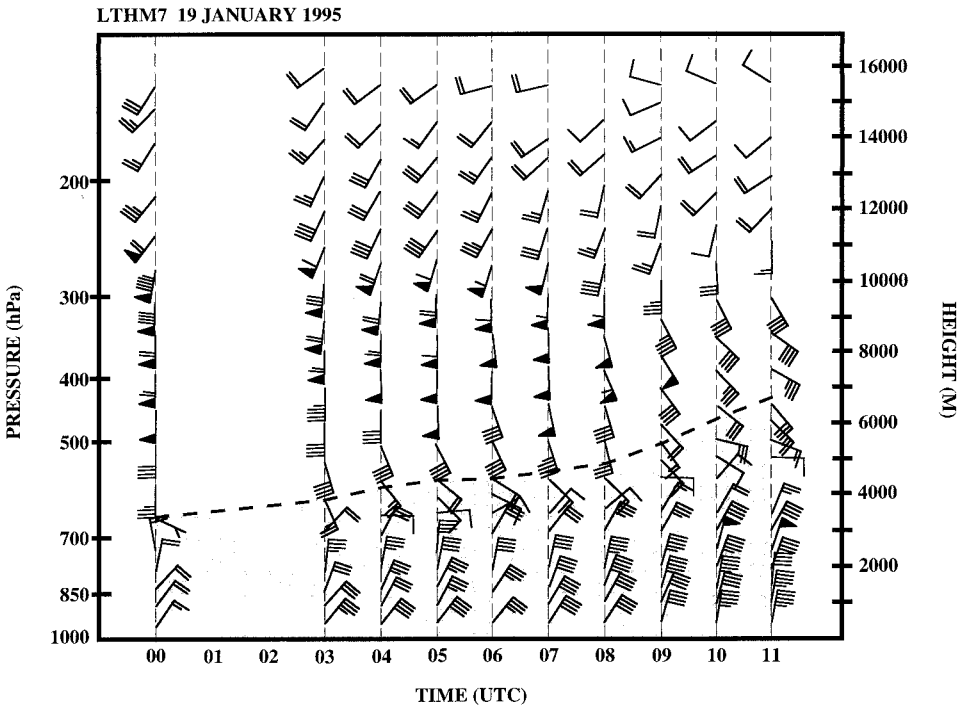

FIG. 6. Time series of winds at the Lathrop, Missouri (LTH), wind profiler taken from 0000 to 1100 UTC 19 January 1995. Wind speed and direction indicated as in Fig. 1a. Dashed line indicates top of a layer of veering winds. The layer of veering winds is shaded.

souri. Such a thermal structure is the classic thermodynamic signature of a warm-occluded system.

Note the cold-air bubble at 850 hPa that, having broken off from the larger pool of cold air in Minnesota, had been rapidly rotated around the developing cyclone to a position directly south of the 850-hPa cyclone center. Its position is testimony to the strength of the circulation associated with this cyclone.

At 700 hPa (Fig. 8c) the thermal field was dominated by the presence of the intensified upper-level front over the Gulf Coast states. This feature coupled with the vertical extension of the surface cold front resulted in a cyclone center at 700-hPa rung by a tight baroclinic gradient on its southern periphery. Little evidence of the warm frontal baroclinic zone or a warm occlusion existed at 700 hPa in the θ analysis. The 700-hPa θ_e analysis (Fig. 9), however, dramatically demonstrates the occluded nature of this cyclonic system. By 0000 UTC 20 January, θ_e at this level had wrapped up into a tight structure with the heavy snow falling along the length of the 700-hPa θ_e warm and occluded fronts.

The upper-level front at 500 hPa (Fig. 8d) over the Gulf Coast states was fully developed by this time. It was accompanied by nearly 50 m s^{-1} winds on its warm edge and nearly 90° of streamline curvature from central Alabama to central North Carolina. As shown by many previous investigators (e.g., Shapiro 1981; Keyser and Shapiro 1986; Martin et al. 1992) when the upper front migrates to the downstream side of the upper trough, it often takes on a thermally direct vertical circulation that is conducive to surface development. Such was the case with the current cyclone as the surface redevelopment in southern Ohio attests.

Figure 10 is a cross section of θ_e through the warm-occluded front at 0000 UTC 20 January. The intersection of the cold-frontal air mass and the warm-frontal air mass is clearly visible just south of Peoria, Illinois (PIA). With reference to Fig. 8a again, the maximum snow intensity was located just northwest of PIA at this time, forming ahead of the upper cold front of the warm occlusion. Model trajectory analysis to be shown in Part II will demonstrate that air parcels experienced maximum ascent in the trowal (trough of warm air aloft) as suggested by Penner (1955) and Galloway (1958) in their three-front model. In section 5 of the present paper, it will further be shown that parcels that had resided in the cold-frontal baroclinic zone for much of their history, rose abruptly upon encountering the warm front; thus, the formation of the *midlevel* occluded structure in this case occurred exactly as suggested in the Norwegian cyclone model with the cold-frontal zone catching up with, and subsequently ascending, the warm-frontal zone.

3. Model description

To further elucidate the frontal structure of this cyclone, output from a successful forecast of the event

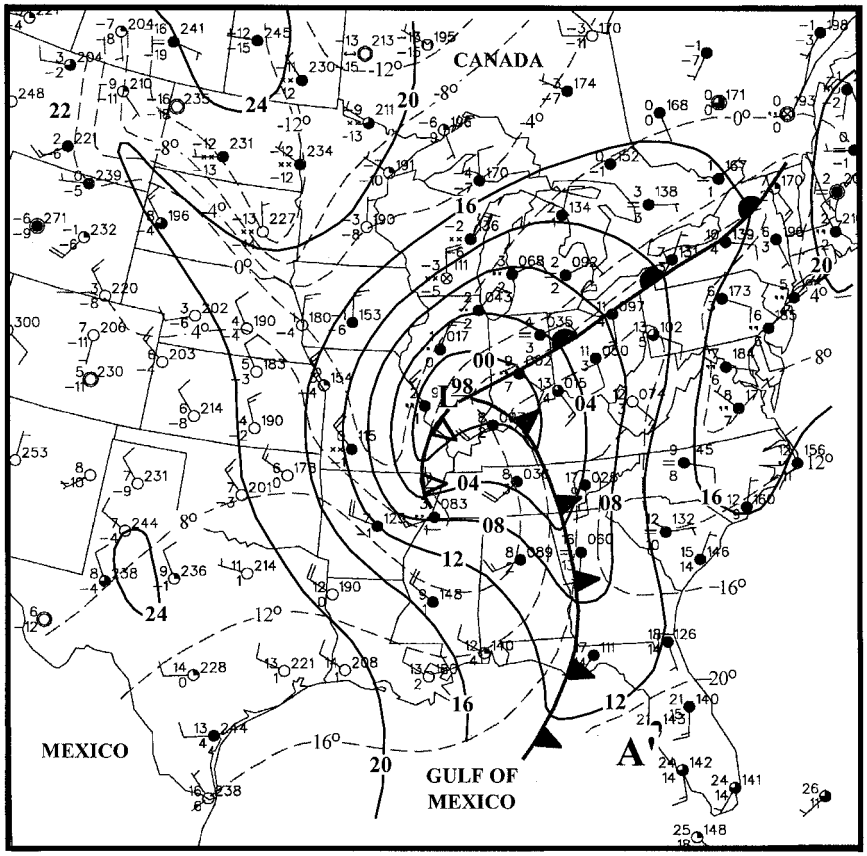

FIG. 7. As in Fig. 1a except for 1800 UTC 19 January 1995.

made using the University of Wisconsin—Nonhydrostatic Modeling System (UW-NMS) is used. UW-NMS is described by Tripoli (1992a) and Tripoli (1992b). The model employs a two-way interactive, moveable nesting scheme, which allows for the simultaneous simulation of large synoptic-scale forcing as well as frontal-scale forcing. Prognostic variables carried by the model include u, v, w, and π (Exner function); ice–liquid potential temperature θ_{il}; and total water mixing ratio, as well as the mixing ratios for a variety of precipitation particles.

Advection of the scalar variables is accomplished using a sixth-order Crowley scheme (Tremback et al. 1987), while the dynamic variables are advected using a second-order enstrophy conserving leapfrog scheme (Sadourny 1975). Model physics include a radiation parameterization that predicts long- and shortwave radiative transfer in a cloudy atmosphere (Chen and Cotton 1983), and a predictive soil model with surface energy budget (Tremback and Kessler 1985). Liquid and ice processes are represented in the model by an explicit microphysics package that describes the evolution of cloud water, rainwater, pristine crystals, snow crystals, aggregate crystals, and graupel (Cotton et al. 1986; Flatau et al., 1989). A version of the Emanuel (1991) convective parameterization was employed, modified such that the convection equilibrates with the cyclone and frontal-scale vertical motion forcing.

Three grids were used in the simulation. Grid 1 (outer grid), grid 2 (middle grid), and grid 3 (inner grid) had horizontal resolutions of 160, 80, and 40 km, respectively. The data from grid 2 was predominantly used in this study. The geographic locations of these grids are shown in Fig. 11.

The model employed geometric height as the vertical coordinate with discretely blocked out topography similar to that used in the National Centers for Environmental Prediction (NCEP) Eta Model. Forty vertical levels were used with the vertical grid spacing of 200 m in the lowest 5 grid levels with a gradual geometric stretching (by a factor of 1.07) above that such that the next 18 levels had an average spacing of 404 m and the top 17 levels had a spacing of 700 m. The model top was located at 19.2 km.

The model was initialized by interpolating directly from the 90.5-km NCEP Eta initialization, which has 50-hPa vertical resolution. Horizontal wind components, geopotential height, temperature, and relative humidity were interpolated horizontally along constant pressure surfaces to the locations of the model grid points. Data were then vertically interpolated to the model grid levels. The lateral boundaries were updated

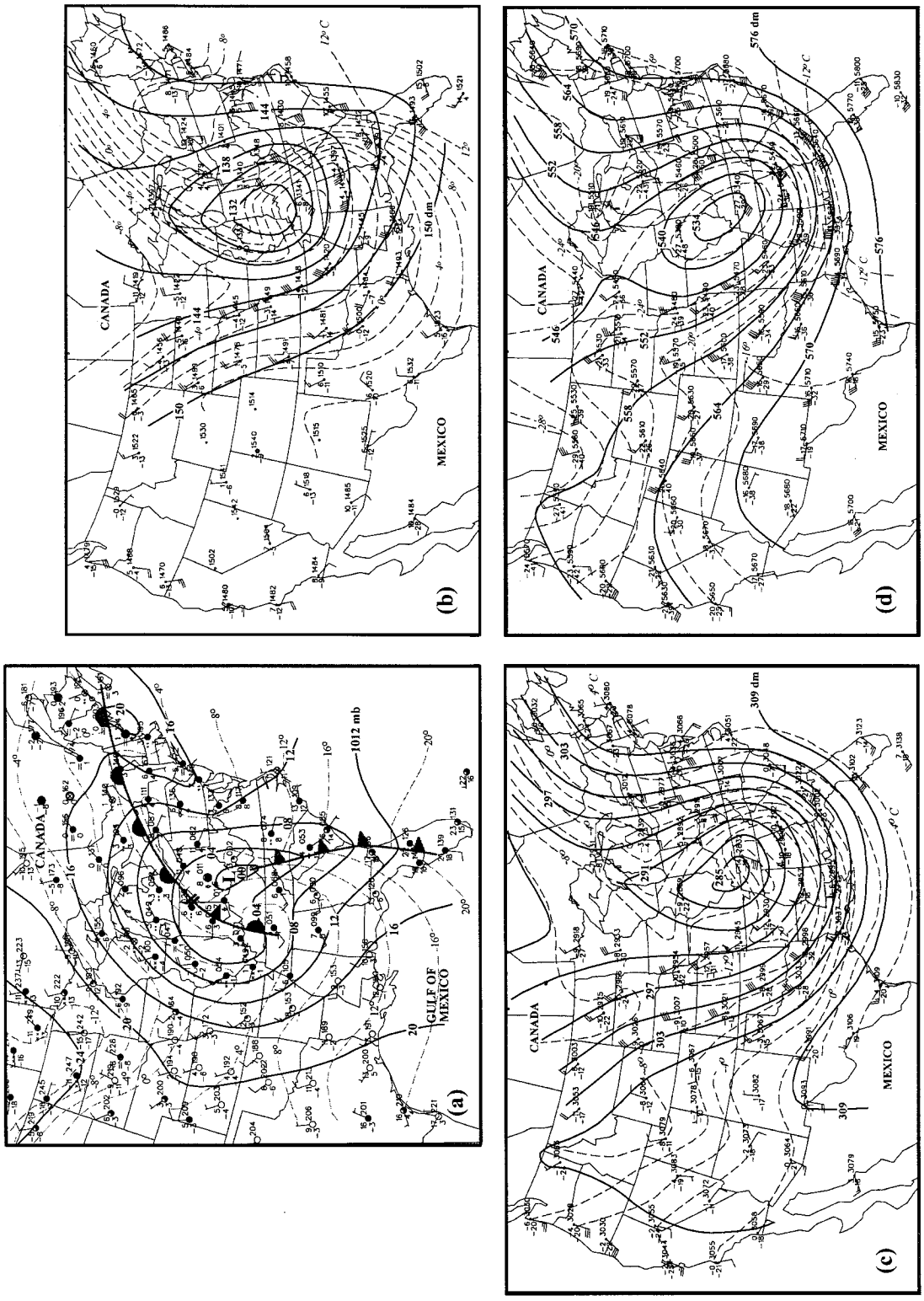

FIG. 8. (a) As in Fig. 1a except for 0000 UTC 20 January 1995. Conventional symbol marks the position of the occluded front. (b) As in Fig. 1b except for 0000 UTC 20 January 1995. (c) As in Fig. 1c except for 0000 UTC 20 January 1995. (d) As in Fig. 1d except for 0000 UTC 20 January 1995.

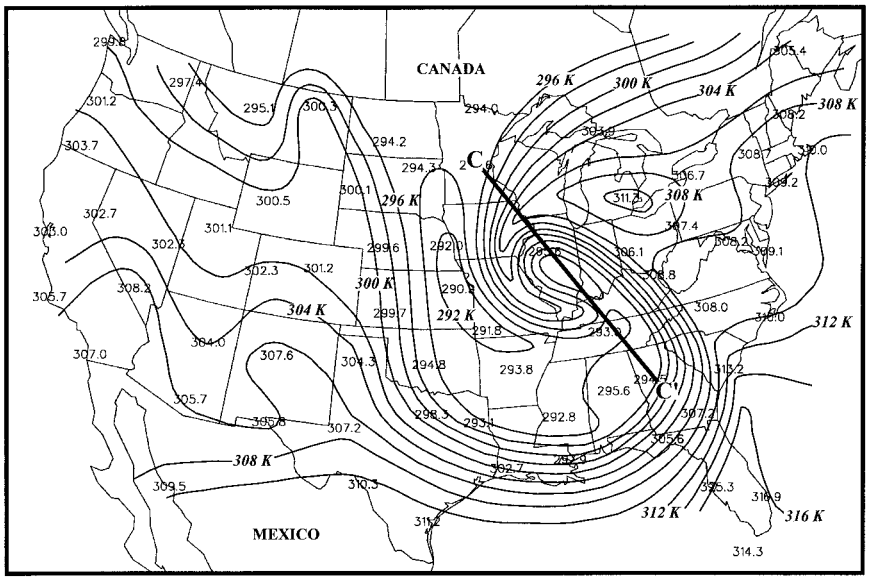

FIG. 9. As in Fig. 4 except for 0000 UTC 20 January 1995. A vertical cross section along line *CC′* is shown in Fig. 10.

every 6 h from the EA gridded forecasts using a Rayleigh-type absorbing layer. The simulation was initialized at 0000 UTC 19 January 1995 and was run for 48 h. Only the first 36 h of this 2-day run are used in this study.

A systematic verification of the model simulation will not be presented here. In subsequent sections of the paper, however, model forecasts will be presented, which, through comparison to the observations presented in the preceding section, will testify to the fidelity of the numerical simulation. Although excellent, the accuracy of the model simulation is not the main focus of this study nor is exact agreement necessary for the purposes of this work. Given this accuracy, we confidently employ the gridded output from this simulation to demonstrate how the occluded structure of this cyclone developed.

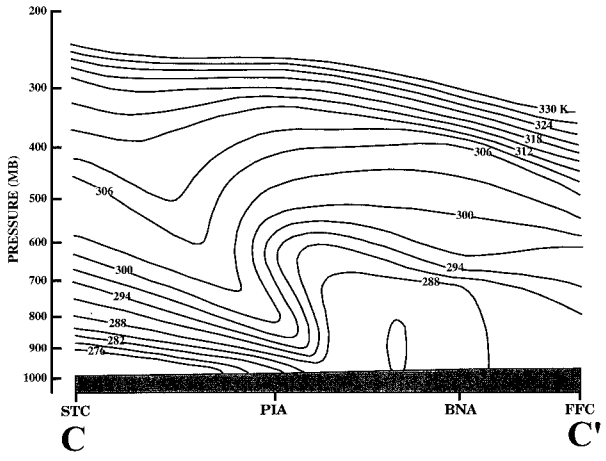

FIG. 10. Vertical cross section, along line *CC′* in Fig. 9, from St. Cloud, Minnesota (STC), to Peoria, Illinois (PIA), to Nashville, Tennessee (BNA), to Peachtree City, Georgia (FFC), at 0000 UTC 20 January 1995. Solid lines are contours of equivalent potential temperature θ_e contoured every 3 K.

4. The occluded frontal structure

a. The warm-occluded front

The nature of the occlusion process has been controversial since the idea was first proposed by Bjerknes

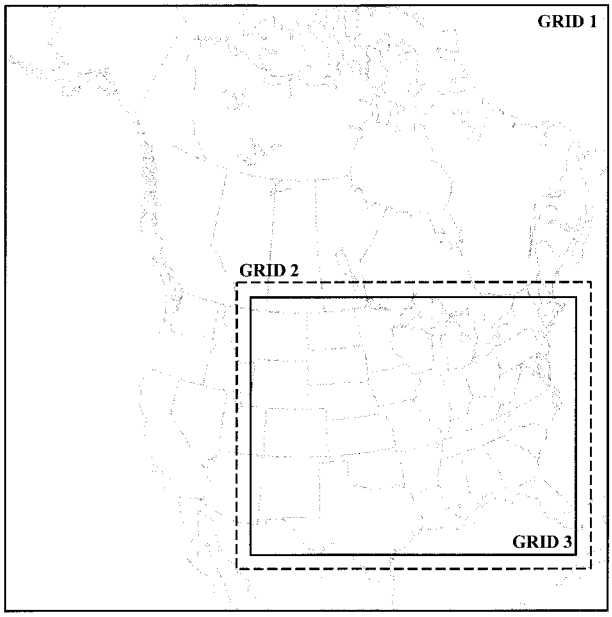

FIG. 11. Geographical locations of the three grids used in the numerical model simulation of this case. Results in this paper use grid 2.

and Solberg (1922) in their seminal paper on the structure and life cycle of extratropical cyclones. In the conceptual model they introduced in that paper (known colloquially as the Norwegian cyclone model), a wavelike disturbance on a deep, preexisting polar front amplified into the cyclone. During this amplification the polar front was distorted into a cold front and a warm front while a region of homogeneous warm air was left between the two surface fronts. This region was known as the *warm sector* and the air there was known as *warm sector air*. The warm occlusion portion of the conceptual model (i.e., the classical warm occlusion) described the vertical displacement of warm sector surface air that resulted from the cold front overtaking, and subsequently ascending, the warm frontal surface. One of the main results of this process was the production of a wedge of warm air aloft displaced poleward of the surface warm-occluded front.

In the late 1950s, scientists at the Canadian Meteorological Service (Godson 1951; Penner 1955; Galloway 1958, 1960) showed that identification of this trowal was of great assistance in describing the important characteristics of warm-occluded cyclones. The trowal is a line connecting the crests of the thermal wave at successive heights (Crocker et al. 1947). Godson (1951) referred to a ''sloping valley of tropical air'' in connection with this idea. Galloway (1958), who named the feature, stated that the ''trowal marks the crest of the warm air aloft.'' As such, the trowal marks the 3D sloping intersection of the upper cold-frontal portion of the warm occlusion with the warm-frontal zone. Importantly, the trowal can exist even without an occluded front beneath it (Godson 1951). The motivation for this analysis tool was the observation that the position of this trowal showed a greater correspondence to the cloud and precipitation features associated with an occluded cyclone than did the small wind and temperature changes associated with the warm occluded front at the surface. Indeed, doubt was expressed as to the very existence of the classical occlusion (Penner 1955).

Recently, the subject of occluded cyclones has enjoyed renewed attention. An outstanding review of previous work on the nature of occluded fronts is given in Schultz and Mass (1993) and will not be repeated here. Such a survey of prior work suggests that the term ''occlusion'' has traditionally been used to refer to one of three things; 1) the postmature *stage* in the life cycle of an individual cyclone, 2) a *process* leading to the decay of a cyclone, or 3) a specific 3D thermodynamic *structure* sometimes observed in cyclones. Such lack of consensus on what is meant by ''occlusion'' has undoubtedly contributed to the controversy surrounding the concept. For instance, several previous studies have documented warm-occluded structures that did not result from the classical process (some of which did not even describe cyclones in their decaying stage) (Douglas 1929; Arakawa 1952; Palmén 1951; Kuo and Reed 1988; Locatelli et al. 1989; Martin et al. 1990; Hobbs et al. 1990; Schultz and Mass 1993; Castle et al. 1996). In the present paper the term ''occluded structure'' will be used to refer to a frontal structure characterized by 1) the horizontal juxtaposition of two baroclinic zones separated by an axis of highest θ or θ_e, and 2) a sloping vertical axis of maximum θ_e extending from the surface to upper-tropospheric levels, that separates two regions of large horizontal θ_e gradient. The term ''occlusion'' will be used to refer to the *process* by which the frontal structure of a cyclone evolves into the ''occluded structure'' previously defined. Relating this frontal evolution to the cyclone life cycle, Schultz and Mass defined ''occlusion'' as a process ''in which the low center becomes progressively separated from the warm sector of a cyclone.'' We agree with this definition and also agree that as a result of this process ''a pressure trough and an associated tongue of intermediate temperature air extends from the low center to the warm sector.'' Within this pressure trough resides the warm-occluded front. (Schultz and Mass restricted their attention to the trough in the *sea level* pressure but their definition is applicable at any level). Therefore, an axis of maximum θ (or θ_e) on a horizontal map (at any level) can be used to indicate the position of the occluded front at that level.

Based on these definitions of ''occluded structure'' and ''occlusion,'' and their attendant structural consequences, analyses of θ_e at the surface at 6-h intervals from 1200 UTC 19 January to 0600 UTC 20 January 1995 from the model simulation are presented in Fig. 12. At 1200 UTC (Fig. 12a) the cold front, warm front, and bent-back front are clearly identifiable as is the region of weak frontal gradient in extreme southwestern Tennessee. The point of intersection between the cold and warm fronts is located at the minimum in sea level pressure. Six hours later (Fig. 12b) the cold front and warm front are still identifiable. A sea level pressure trough has developed southwestward along the bent-back front. By 0000 UTC 20 January a warm-occluded front had developed at the surface (Fig. 12c). A weak but well-defined ridge of high θ_e connects the surface occluded front, that runs from northeastern Illinois to western Kentucky, to the peak of the warm sector. The point of intersection between the occluded front and the peak of the original warm sector is defined as the *triple point.* The weak sea level pressure trough, previously associated with the bent-back front, remained located to the southwest of the triple point along what was now the surface occluded front. At 0600 UTC (Fig. 12d) the axis of maximum θ_e remained clearly evident and a minimum in sea level pressure (in the model simulation) continued to appear at the end of the occluded front over southern Illinois and Indiana.

Often neglected in studies of occluding cyclones is a description of their middle tropospheric frontal structure. In Fig. 13 analyses of pressure and θ_e at 6-h intervals at a geopotential height of 2 km are presented. The 2-km pressure and θ_e structure at 1200 UTC (Fig. 13a) resembled its sea level counterparts at 1800 UTC

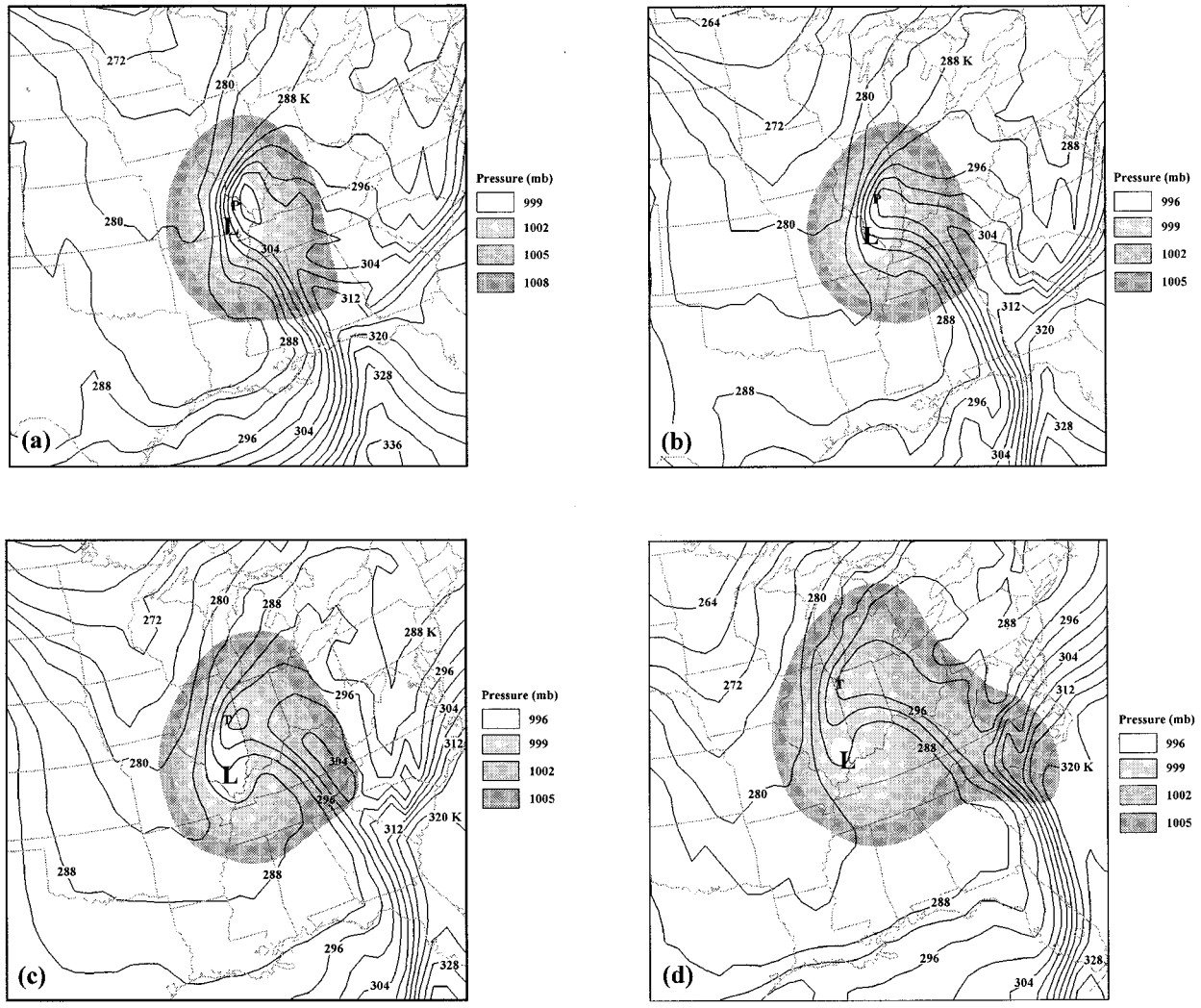

FIG. 12. (a) The 12-h forecast of sea level pressure and surface θ_e, valid at 1200 UTC 19 January 1995, produced by the UW-NMS model simulation. Shading represents sea level pressure at 3-hPa intervals (legend is to the right). Solid lines are contours of surface equivalent potential temperature θ_e contoured every 4 K. The ''P'' represents the position of the peak of the warm sector. (b) As in Fig. 12a except for 18-h forecast valid at 1800 UTC 19 January 1995. (c) As in Fig. 12a except for 24-h forecast valid at 0000 UTC 20 January 1995. The ''T'' represents the position of the triple point. (d) As in Fig. 12c except for 30-h forecast valid at 0600 UTC 20 January 1995.

with a slight indication of a ridge of high θ_e extending southward from the intersection of the cold and warm fronts. The pressure minimum at this level was clearly located to the southwest of this intersection along the bent-back front. At 1800 UTC a clear occluded frontal structure is indicated extending southwestward from Chicago to southeast Missouri where the pressure minimum existed (Fig. 13b). Six hours later, at 0000 UTC 20 January, an extraordinary extension of the occluded front was evident (Fig. 13c). The pressure minimum was located far to the south-southwest of the triple point, which was over Lake Michigan. By 0600 UTC (Fig. 13d) the cold front had moved rapidly eastward and the occluded front had taken on a more meridional orientation with a slight increase in length. Very little θ_e advection occurred along the occluded front at this time. The apparent retreat of high-θ_e air back toward the original warm sector evidenced in Fig. 13 is not a result of general cooling or drying of the air being processed by the occluded structure. Instead it is evidence that the air was being lifted upward, away from the 2 km surface, during (and as a result of) the occlusion process.

It is apparent from a comparison of Figs. 12b and 13a that the cyclone developed a warm-occluded structure at upper levels earlier than it did at the surface. Both the surface at 1800 UTC (Fig. 12b) and the 2-km surface at 1200 UTC (Fig. 13a) show the incipient development of a ridge of high θ_e in the horizontal. The development of this structure occurred at least 6 h earlier at 2 km than it did at the surface. The possible reasons for the asynchronous development of the warm-occluded structure will be discussed in section 5.

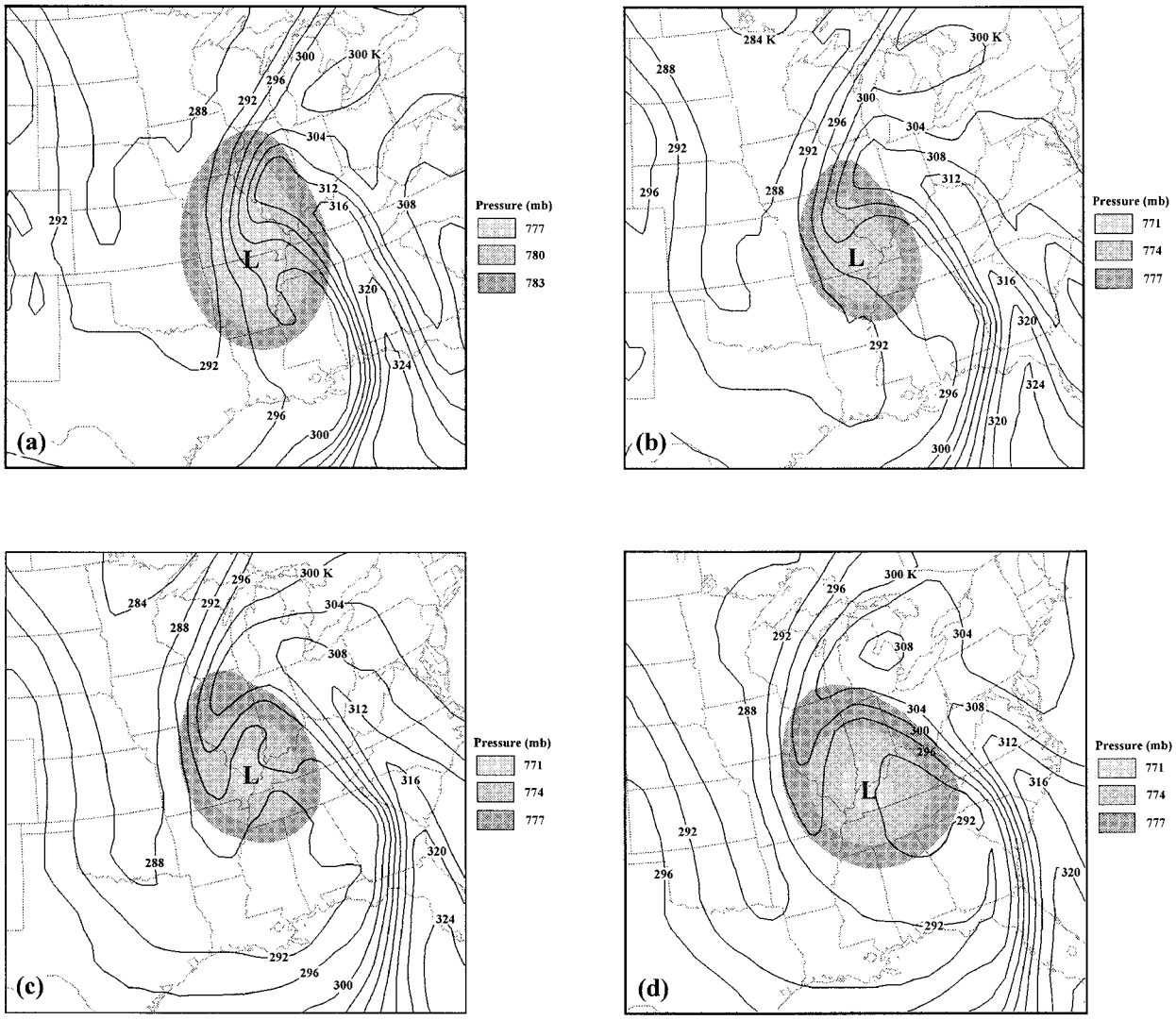

FIG. 13. (a) The 12-h forecast of pressure and θ_e, valid at 1200 UTC 19 January 1995, on the 2.03-km geopotential height surface produced by the UW-NMS model simulation. Shading represents pressure contoured every 3 hPa with legend to the right. Solid lines are contours of equivalent potential temperature θ_e at 2.03 km contoured every 3 K. (b) As in Fig. 13a except for 18-h forecast valid at 1800 UTC 19 January 1995. (c) As in Fig. 13a except for 24-h forecast valid at 0000 UTC 20 January 1995. (d) As in Fig. 13a except for 30-h forecast valid at 0600 UTC 20 January 1995.

b. Topography of the occluded structure

Thus far, it has been shown that the 19 January cyclone did develop an occluded structure although the timing of the development varied in the vertical; appearing first at midtropospheric levels and then at the surface. In this section some of the morphological characteristics of the 309-K θ_e surface are examined. Selection of the 309-K θ_e surface is not arbitrary but instead is based on the fact that in numerous model cross sections this surface was located near the warm edge of both the warm-frontal and cold-frontal zones.

Topographic maps of this surface at 6-h intervals from 0000 UTC 19 January to 0600 UTC 20 January are shown in Fig. 14. At 0000 UTC 19 January (Fig. 14a), the portion of this surface that extends from southwest Arkansas into the Gulf of Mexico constitutes the cold-frontal portion of the surface. Notice that the eastern edge of this portion of the surface has extremely steep slope. The portion of the surface that begins in central Arkansas and has shallower slope extending into Kansas, Iowa, Wisconsin, and Minnesota is the warm-frontal portion of this surface. Some of the higher elevation contours exhibit a slight kink at the point where the warm-frontal portion of the surface meets the cold-frontal portion of the surface in extreme northeastern Oklahoma (Fig. 14a). By 0600 UTC (Fig. 14b), the result of significant cyclonic curling of the θ_e surface is evident in northwestern Arkansas. By this time the cold-frontal

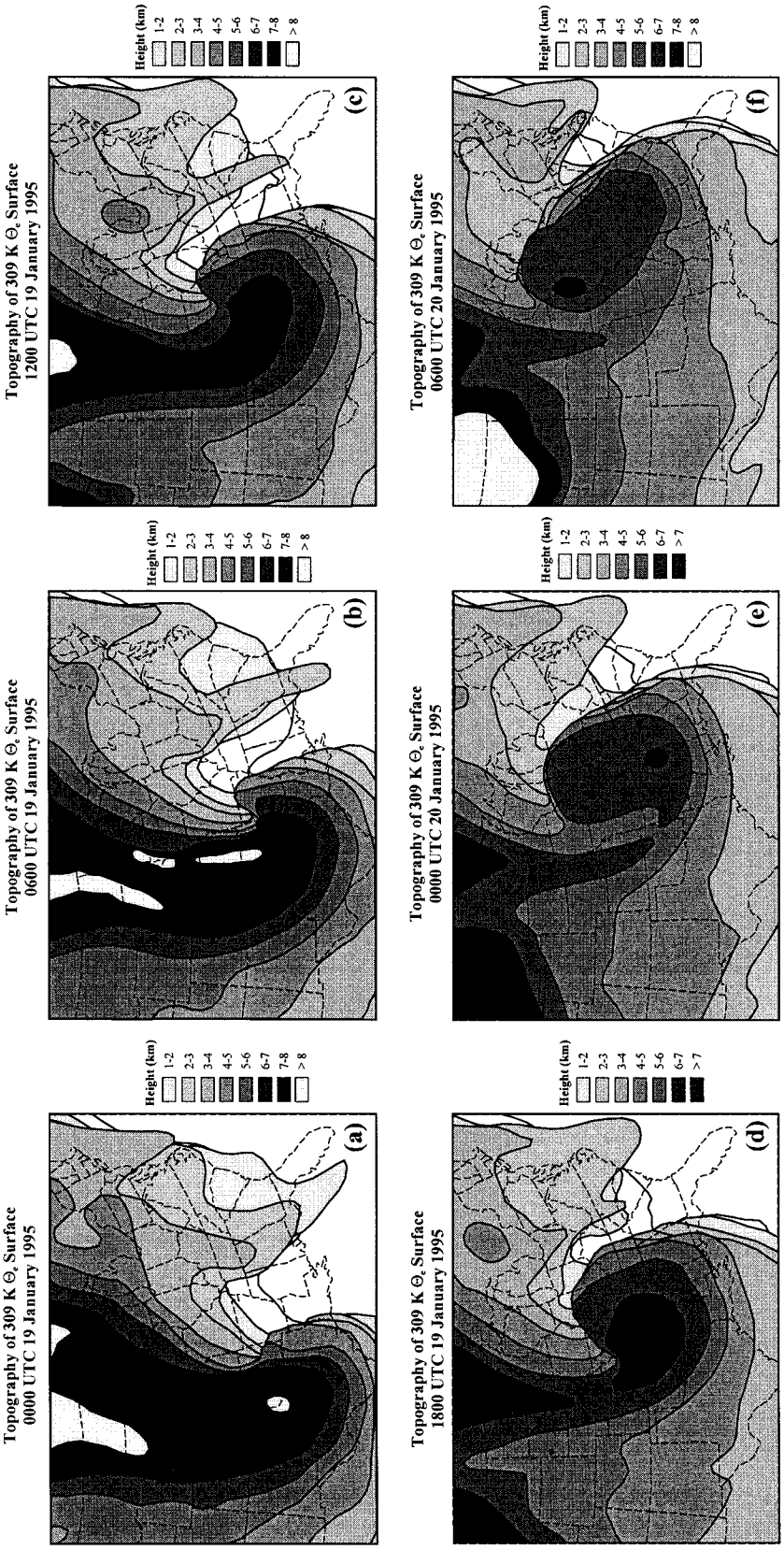

FIG. 14. (a) Topography of the 309-K θ_e surface at 0000 UTC 19 January from the 0-h forecast of the UW-NMS model simulation. Height of the 309-K θ_e surface is contoured every 1 km with legend on the right. (b) As in Fig. 14a except from a 6-h forecast valid at 0600 UTC 19 January 1995. (c) As in Fig. 14a except from a 12-h forecast valid at 1200 UTC 19 January 1995. (d) As in Fig. 14a except from an 18-h forecast valid at 1800 UTC 19 January 1995. (e) As in Fig. 14a except from a 24-h forecast valid at 0000 UTC 20 January 1995. (f) As in Fig. 14a except from a 30-h forecast valid at 0600 UTC 20 January 1995.

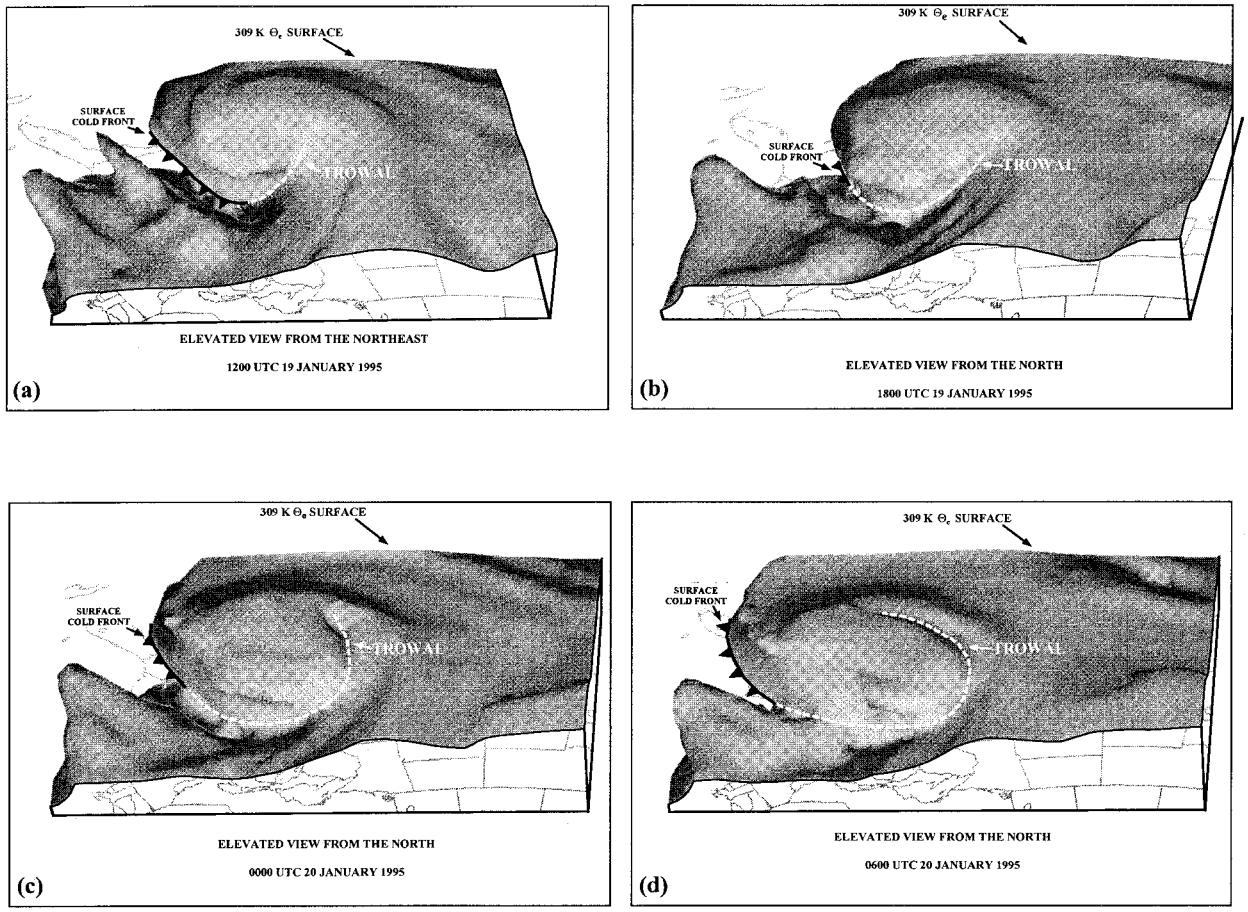

FIG. 15. (a) Elevated, northern view of the 309-K θ_e isentropic surface from a 12-h forecast of the UW-NMS model valid at 1200 UTC 19 January 1995. Cold-frontal symbol indicates the position of the surface cold front. Dashed line indicates position of the trowal (see text for explanation). (b) As in Fig. 15a except from an 18-h forecast valid at 1800 UTC 19 January 1995. (c) As in Fig. 15a except from a 24-h forecast valid at 0000 UTC 20 January 1995. (d) As in Fig. 15a except from a 30-h forecast valid at 0600 UTC 20 January 1995.

portion of the surface extended as far east as western Mississippi and as far north as the Missouri–Arkansas border. The warm-frontal portion of the surface intersected the ground in northeastern Arkansas and was steeply sloped into Kansas, Nebraska, and Minnesota. The cyclonic curling continued noticeably to 1200 UTC 19 January (Fig. 14c) at which time there appeared to be some folding over of the cold-frontal portion of this θ_e surface with the northeast–southwest-oriented warm-frontal portion of the surface. Of particular interest is the notch in the topography that pokes upward from low levels over east-central Missouri to central Missouri. This ''canyon'' in the 309-K surface is more dramatically evident at 1800 UTC (Fig. 14d) by which time the cyclonic curling of the surface had resulted in the cutting off of the 7-km isoline. The sloping canyon extended upward toward west-central Missouri at this time. By 0000 UTC 20 January (Fig. 14e) there was so much folding over between the cold-frontal and warm-frontal portions of this surface that the plan view perspective fails to be informative except in showing that the sloping canyon of low elevations had become much longer, extending from the Ohio Valley to extreme southwest Missouri. The situation was even more extreme by 0600 UTC 20 January (Fig. 14f). Throughout the 30-h period, this θ_e surface had been cyclonically rotated to the point where the highest elevations had been wrapped over lower elevations and a somewhat isolated vortex of high-elevation (i.e., low-) θ_e air had been cut off from the high latitude reservoir of low-θ_e air.

A 3D perspective view of the wrapping up of the 309-K θ_e surface is given in Fig. 15, which shows a series of 309-K θ_e isosurfaces, at 6-h intervals, as viewed from a northerly and slightly elevated perspective. At 1200 UTC 19 January (Fig. 15a), a surface cold-frontal symbol marks the intersection of the 309-K θ_e surface with the physical surface of the earth. There is also a 3D sloping intersection of the dome of low θ_e (i.e., the cold-frontal zone) over the less steeply sloped warm-frontal zone of θ_e. This intersection is precisely the trowal described earlier. The trowal represents the

3D sloping ''canyon'' in the 309-K surface described with reference to Fig. 14 and is reminiscent of the ''sloping valley of tropical air'' referred to by Godson (1951) in his work on occluded cyclones. By 1800 UTC 19 January (Fig. 15b) the trowal had elongated at the expense of the surface cold front. This trend continued through 0600 UTC 20 January (Figs. 15c and 15d) at which time the trowal rung the region of 7-km elevation seen in Fig. 14f. It is clear upon inspection of the hourly evolution of this surface (not shown here[1]) that the intersection of the cold-frontal and warm-frontal zones occurred first at midtropospheric levels on the θ_e surface and progressively worked its way downward to lower elevations. This behavior is consistent with the inferences made regarding the formation of the occluded structure of this storm from examination of Figs. 12 and 13. Thus, the formation of the occluded structure in this case was initiated at midtropospheric levels and then proceeded downward toward the surface. This structure also appeared to involve the sloping vertical intersection of previously identifiable cold- and warm-frontal zones.

5. Formation of the warm-occluded structure

The vertically asynchronous development of the warm-occluded structure in this case was documented in the previous section. In this section air parcel trajectories calculated from the UW-NMS model output are used to separately investigate the formation of the warm-occluded structure near the surface and at midtropospheric levels. We begin with an investigation of the development of the warm-occluded structure near the surface.

a. Development of the surface warm occlusion

Figure 16 shows surface θ_e at 3-h intervals from 1800 UTC 19 January to 0300 UTC 20 January. There is barely a hint of a horizontal axis of maximum θ_e at 1800 UTC (Fig. 16a). By 2100 UTC, however, an axis of maximum θ_e can be seen stretching from southcentral Illinois toward southeast Missouri (Fig. 16b). This synoptic feature is very clearly evident by 0000 and 0300 UTC 20 January (Figs. 16c and 16d). Since the axis of maximum θ_e is the warm-occluded front at the surface, trajectory analysis is used to investigate the creation of this feature.

A large number of trajectories traced backward in time and space from approximately 140 m MSL at 0000 UTC 20 January were examined. These trajectories experienced negligible vertical motion over the 24-h period. Rather than present all of these trajectories, five representative ones that were involved in the production of the warm-occluded structure at the surface are shown in Fig. 17. Trajectory A in Fig. 17 is representative of air that originated from behind or within the cold frontal zone at 0000 UTC 19 January. This air circled cyclonically around the sea level pressure minimum and eventually moved northward through Kentucky and southern Illinois. During the cyclone's evolution, the airstream represented by trajectory A became confluent with an airstream that originated in the warm sector, represented by trajectory B. The confluence of these airstreams for a portion of their histories is reflected in the 200-m frontogenesis pattern displayed in Fig. 18. Trajectories A and B became parallel in northern Alabama after about 1800 UTC (at which time a frontogenesis maximum existed there). Parcel B remained just east of the cold-frontal zone after that time and A and B then proceeded northward. The lack of horizontal confluence after 1800 UTC rendered the cold front frontogenetically inactive. It was this frontogenetically inactive baroclinic zone, the historical surface cold front, that formed the southeastern border to the axis of maximum θ_e defining the surface warm occlusion. The gradual weakening of the frontogenesis in the northern portion of the cold-frontal zone, which evolved to the point where a significant fracture in the frontogenesis occurred by 1800 UTC (Figs. 18c–e), is similar to what Schultz and Mass (1993, their Fig. 14) observed in their study of an occluding continental cyclone.

The baroclinic zone that formed the northwestern border of the axis of maximum θ_e was the result of significant horizontal confluence between warm-frontal trajectories (C and E in Fig. 17) and warm sector trajectories (D). Streams of air both from within (trajectory C) and poleward of (trajectory E) the original warm frontal zone were met along their entire southwestward paths by an easterly flow of warm sector air (trajectory D). The frontogenesis that resulted from this horizontal confluence (Fig. 18) maintained the vigor of the warm-frontal zone. In fact, the warm frontogenesis region was fairly stationary from 1800 UTC 19 January to 0600 UTC 20 January (Figs. 18c–e) suggesting that any frontogenesis that occurred along the surface warm-occluded front resulted from the same frontogenetic processes that had historically been sustaining the warm front. Thus, we suggest that the surface warm-occluded front in this case is not a new front as suggested by Wallace and Hobbs (1977) but is an artifact of the horizontal juxtaposition of historical warm and cold fronts, one of which (the warm front) remained frontogenetically active after the development of the warm-occluded structure. This conclusion seems in agreement with one reached by Nieman and Shapiro (1993) and Schultz and Mass (1993); the latter having stated that ''a single frontogenesis feature supports both the warm and occluded fronts.'' We suggest further that the frontogenesis apparently associated with the occluded front is really a

[1] A video animation of the model-derived hourly evolution of the 309-K θ_e surface illustrating the development of the warm occlusion in this case is available for inspection at the World Wide Web site http://marrella.meteor.wisc.edu/occlusion.html.

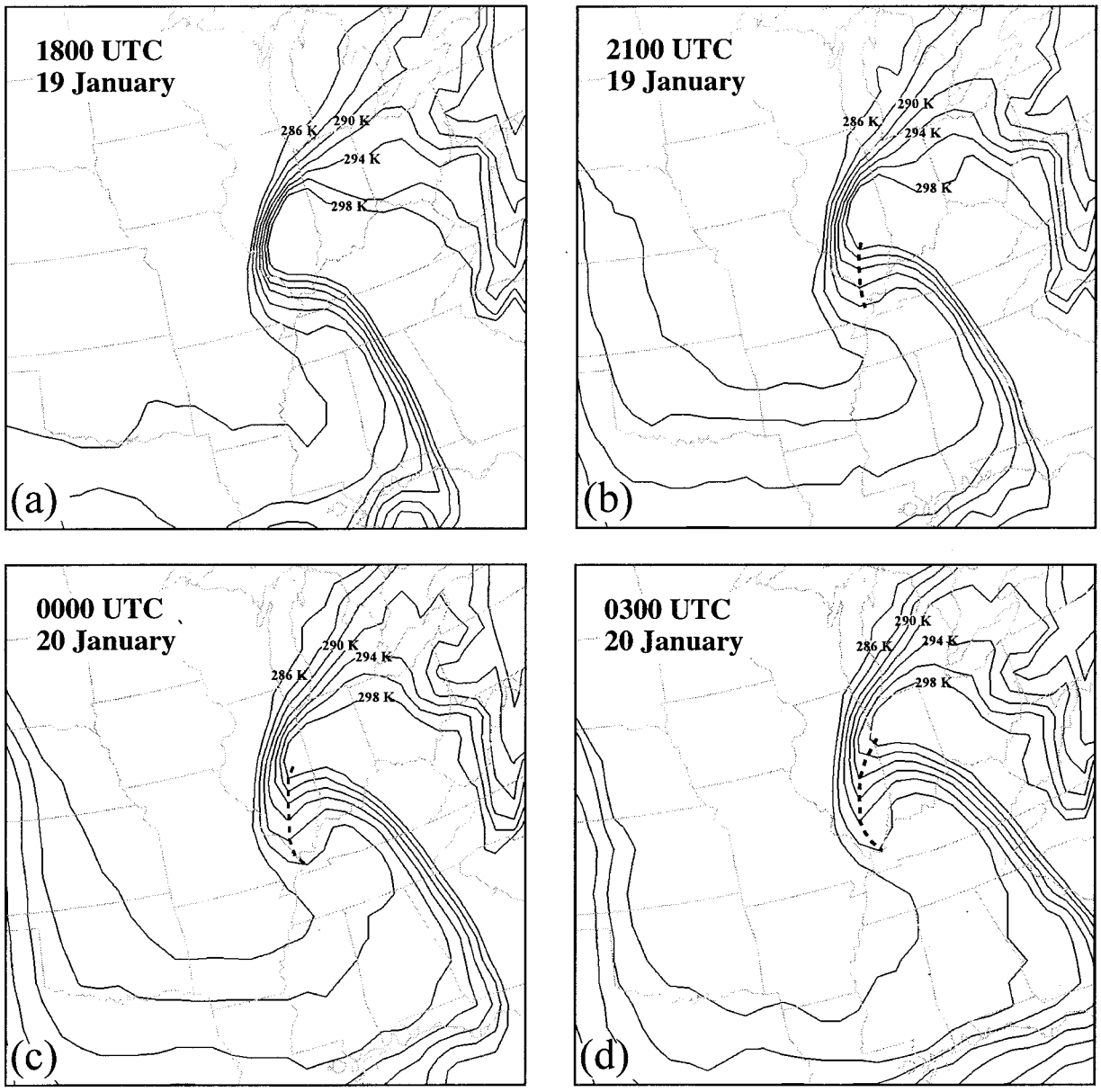

FIG. 16. (a) The 18-h forecast of surface equivalent potential temperature θ_e (from 286 to 298 K contoured every 2 K) valid at 1800 UTC 19 January 1995. (b) As in Fig. 16a except from a 21-h forecast valid at 2100 UTC 19 January 1995. Dashed line indicates axis of maximum θ_e characteristic of warm-occluded front. (c) As in Fig. 16b except from a 24-h forecast valid at 0000 UTC 20 January 1995. (d) As in Fig. 16b except from a 27-h forecast valid at 0300 UTC 20 January 1995.

continuation of the same frontogenesis processes associated with the historical warm front.

The trajectory analysis just presented implies, in agreement with the results of Schultz and Mass (1993), that the formation of the warm-occluded front at the surface results from the cold-frontal baroclinic zone ''catching up'' with the warm frontal baroclinic zone in response to the kinematics of the low-level flow. Since the above analysis concerned motions very near the surface, the restriction of zero vertical velocity precluded an analysis of frontal vertical displacements and their role in the occlusion process. We now proceed to an investigation of the development of the warm-occluded structure in the middle troposphere where no such restriction applies.

b. Development of the midlevel warm-occluded structure

In this section a representative air parcel trajectory that was involved in the formation of the warm-occluded structure at midtropospheric levels is shown. The hor-

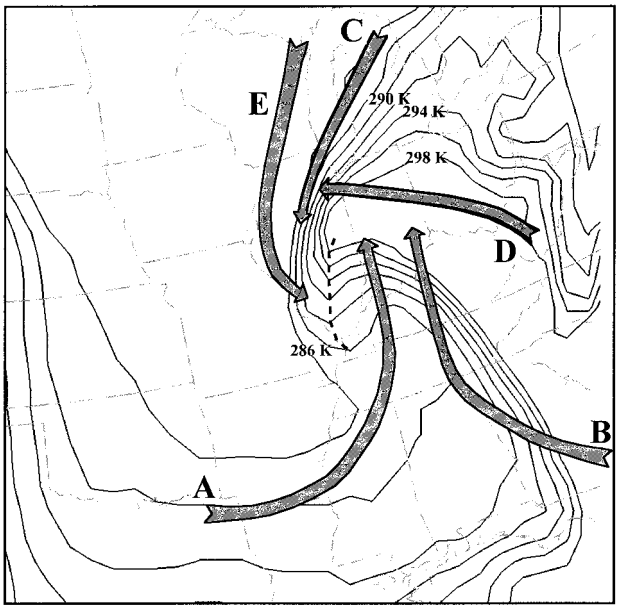

FIG. 17. Representative 24-h absolute trajectories of air parcels involved in the development of the surface warm-occluded structure. Arrows (labeled A, B, C, D, and E) represent different trajectories ending at approximately 140 m at the respective arrowheads at 0000 UTC 20 January 1995 (see text for explanation). Solid lines are contours of surface θ_e at 0000 UTC 20 January (contoured every 2 K from 286 to 298 K). Dashed line is the axis of maximum surface θ_e.

izontal path of the present trajectory is shown in Fig. 19a. It moved rapidly northward from southwest coastal Louisiana into central Illinois by approximately 1500 UTC 19 January. During this time the parcel experienced negligible vertical displacement as can be ascertained by inspection of Fig. 19b. After 1500 UTC, the parcel turned cyclonically, rising from 2–7 km as it did so (Fig. 19b), and moved along the cross section marked *DD′* in Fig. 19a until approximately 0100 UTC 20 January. At 0100 UTC, the parcel turned cyclonically again and headed to the southeast toward the bootheel of Missouri while undergoing gentle descent. It is interesting to note that the beginning of the ascent was coincident with the cyclonic turning in the horizontal as was the beginning of the descent.

The ensuing analysis takes advantage of the fact that this representative parcel remained along the cross section for so long during its ascent. Figure 20 is a series of model cross sections of θ_e along *DD′* at 3-h intervals from 1600 UTC 19 January to 0100 UTC 20 January. The position of the representative parcel is marked by the forwardmost black dot in each panel. The gray shading represents regions of horizontal cold-air advection in the cross section at each time. At 1600 UTC (Fig. 20a) the parcel was clearly located near the front edge of the region of horizontal cold-air advection. It was also near the high-θ_e edge of a noticeable horizontal θ_e gradient. Given that the parcel had moved purely horizontally for the previous 15 h of its trajectory, we conclude that this parcel was located near the warm edge of the cold-frontal zone. The axis of maximum θ_e precisely divided the occluded structure into a region of horizontal cold-air advection associated with the cold-frontal zone and a region of horizontal warm-air advection associated with the warm-frontal zone. Note also that while a warm-occluded structure is evident at and above 2 km in Fig. 20a, no such structure is apparent at the surface.

Three hours later at 1900 UTC (Fig. 20b), the parcel had risen from its original position and yet remained within the cold-frontal zone while quasi-conserving its original value of θ_e. By 2200 UTC (Fig. 20c) even greater ascent had occurred and still the parcel remained within the cold-frontal zone, nearly conserving θ_e as it rose. At this time, the warm-occluded structure finally appears at the surface. By 0100 UTC 20 January (Fig. 20d), the parcel had risen 5 km and yet remained in the cold-frontal zone (although it was more difficult to discern such a zone at that altitude). Throughout the 9-h period, the axis of maximum θ_e characteristic of the warm-occluded structure remained the dividing line between horizontal cold- and warm-air advections. This parcel trajectory, which is representative of many others in the lower and middle troposphere, provides dramatic evidence that, at midtropospheric levels in this case, the cold-frontal air overtook, and subsequently ascended, the warm-frontal surface. Since the cold-frontal zone is composed of cold-frontal air parcels, this suggests that the cold-frontal zone ascended the warm frontal zone in this case. Thus, the formation of the *midlevel* warm-occluded structure exhibited by this storm was a result of the cold-frontal zone gradually encroaching upon, and subsequently ascending over, the warm-frontal zone; consistent with the mechanism proposed by the Bergen School 75 years ago.

6. Discussion

As first formulated by Bergeron and reported by Bjerknes and Solberg (1922), occlusion was thought to be a process, occurring in the postmature stage of the cyclone life cycle, by which the surface cold front rotates around the developing low center and overtakes the warm front. As a consequence of this circumstance, the intervening warm sector air was forced aloft. The occluded front was defined as the surface where the two fronts met. This simple idea has remained controversial since its initial suggestion. In recent work, finescale numerical simulations have been employed to elucidate the process by which occluded structures develop in cyclones.

Kuo et al. (1992) examined the development of a low-level occluded front that was a component of the explosively deepening *Ocean Ranger* storm. They found that the occluded front was confined to levels below 750-hPa and was formed, not through a juxtaposition

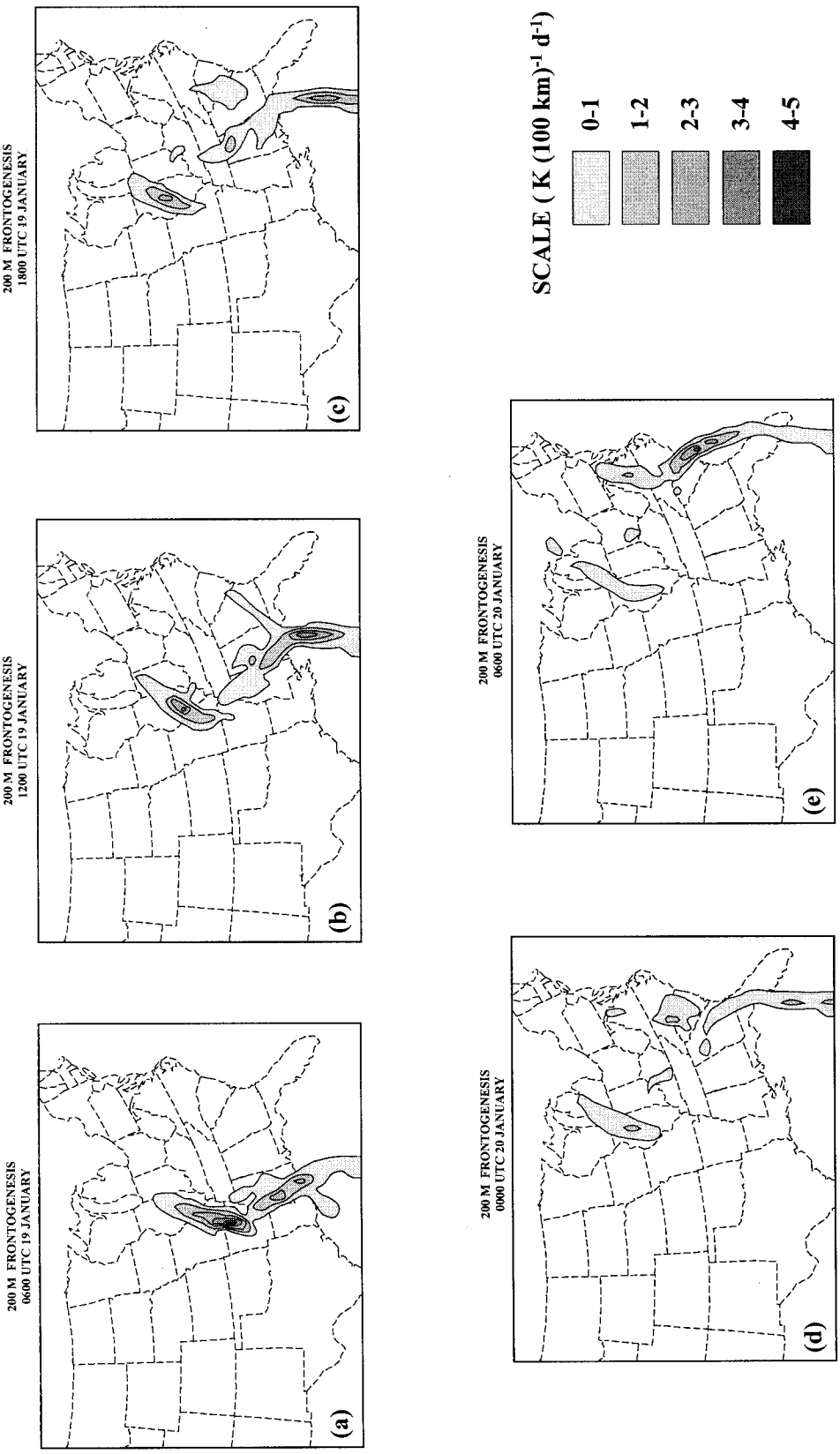

FIG. 18. (a) The 6-h forecast of 200-m frontogenesis from the UW-NMS model valid at 0600 UTC 19 January 1995. Shaded regions are positive frontogenesis regions contoured every 1 K (100 km)$^{-1}$ day^{-1} with legend at lower right. (b) As in Fig. 18a except from a 12-h forecast valid at 1200 UTC 19 January 1995. (c) As in Fig. 18a except from an 18-h forecast valid at 1800 UTC 19 January 1995. (d) As in Fig. 18a except from a 24-h forecast valid at 0000 UTC 20 January 1995. (e) As in Fig. 18a except from a 30-h forecast valid at 0600 UTC 20 January 1995.

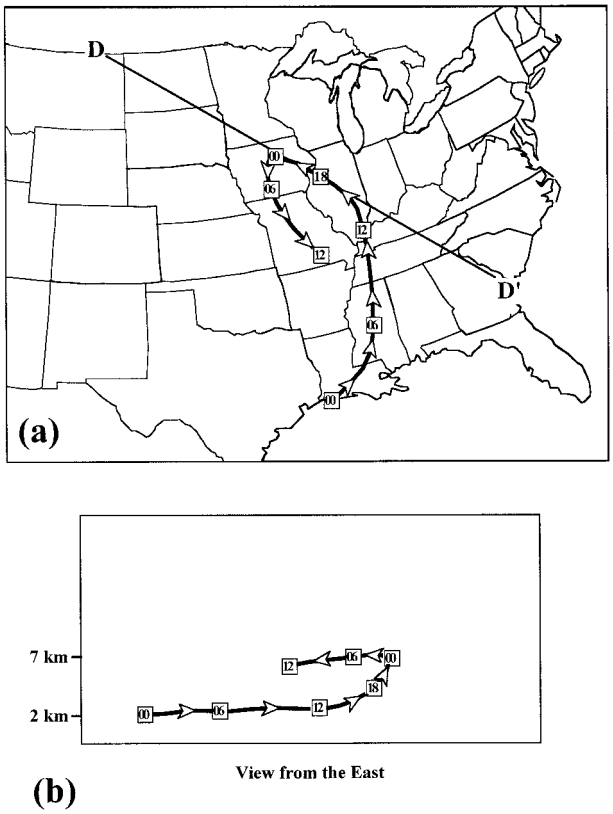

FIG. 19. (a) Plan view of air parcel trajectory involved in formation of the midlevel occluded structure. Boxes with numbers indicate position of the parcel at the indicated time, arrows indicate direction of movement of parcel. A series of vertical cross sections along *DD′* are shown in Fig. 20. Note the parcel trajectory remains along *DD′* from about 1500 UTC 19 January to 0100 UTC 20 January 1995. (b) View from the east of the same air parcel trajectory as in Fig. 19a. Boxes with numbers indicate position of parcel at the indicated time. Height scale is on the left.

of the initial cold and warm fronts, but entirely from air that prior to occlusion was located in the baroclinic zone poleward of the warm front. They noted, however, that as a result of this process warm sector air was forced aloft in agreement with the classical model.

In their study of an explosively deepening continental cyclone, Schultz and Mass (1993) found, in agreement with the classical model, that the surface-occluded front resulted from the steady encroachment of the surface cold front upon the surface warm front. However, they reported that the surface cold front did not *ascend* the surface warm front as suggested in the classical paradigm. Further, the development of the midlevel occluded structure in their case resulted from the intersection of an upper-level front with the surface-based warm-frontal zone. The development of this structure did not involve the vertical displacement of one frontal zone over another.

The present case resembles the classical occlusion process in some respects and contradicts it in others. For instance, the surface occlusion forms as a result of a juxtaposition of the surface cold and warm fronts in agreement with the classical model. At midlevels, the warm-occluded structure formed as a result of the cold-frontal zone encroaching upon, and subsequently ascending, the warm-frontal zone, as suggested by the classical model. However, it was also found that the occluded structure appeared first aloft and later at the surface, in marked contrast to the Bergen school ideas. Still, this case represents the first documentation of a cold-frontal zone encroaching upon, and subsequently ascending, a warm-frontal zone to produce an occluded structure. It is important to note that this mechanism occurred only at midlevels and so *did not* account for the entire 3D development of the occluded frontal structure that characterized this cyclone.

The frontal structure of the 19 January cyclone is also intriguing in that it was characterized by the presence of a shallow bent-back front to the southwest of the sea level pressure minimum while also exhibiting many characteristics of the Norwegian warm occlusion. Recent work concerning the variety of frontal structures that can be associated with midlatitude cyclogenesis (Hoskins 1990; Davies et al. 1991; Thorncroft et al. 1993) has suggested that the frontal structure of idealized baroclinic disturbances is highly sensitive to the amount and sign of the barotropic shear characterizing the cyclogenetic environment. Cyclonic barotropic shear favors the formation of cutoff cold air pools aloft while tending to sustain surface warm fronts at the expense of surface cold frontogenesis (Davies et al. 1991). Following Davies et al. (1991) and Thorncroft et al. (1993), Shapiro and Donall Grell (1994) proposed that such cyclonic shear favors the production of cyclones with the classical warm-occluded structure but with very little ascending motion along the surface-occluded front (which they refer to as the bent-back/occluded front). Conversely, the case of zero (or near zero) barotropic shear favors the production of cyclones with the Shapiro and Keyser (1990) T-bone frontal structure (as in the ERICA IOP 4 storm) with considerable ascent along the bent-back front. Shapiro and Donall Grell (1994) further suggest that this important barotropic shear is made manifest in the real atmosphere through differing vertical and horizontal alignments of the subtropical jet with the polar jet (see their Fig. 19). When the subtropical jet axis lies south (north) of the polar jet axis, the barotropic shear of the cyclogenetic environment is cyclonic (anticyclonic).

In the present case the subtropical and polar jets were nearly vertically coincident after 1200 UTC 19 January. Thus, according to the idealized model results, this case should have favored the formation of the T-bone structure and *not* the warm-occluded structure. Instead, elements of both were present: the classical warm-occluded structure formed in a cyclone that initially exhibited a bent-back frontal structure, and considerable precipitation fell along the bent-back/occluded front. Such a combination of cyclone–frontal structure char-

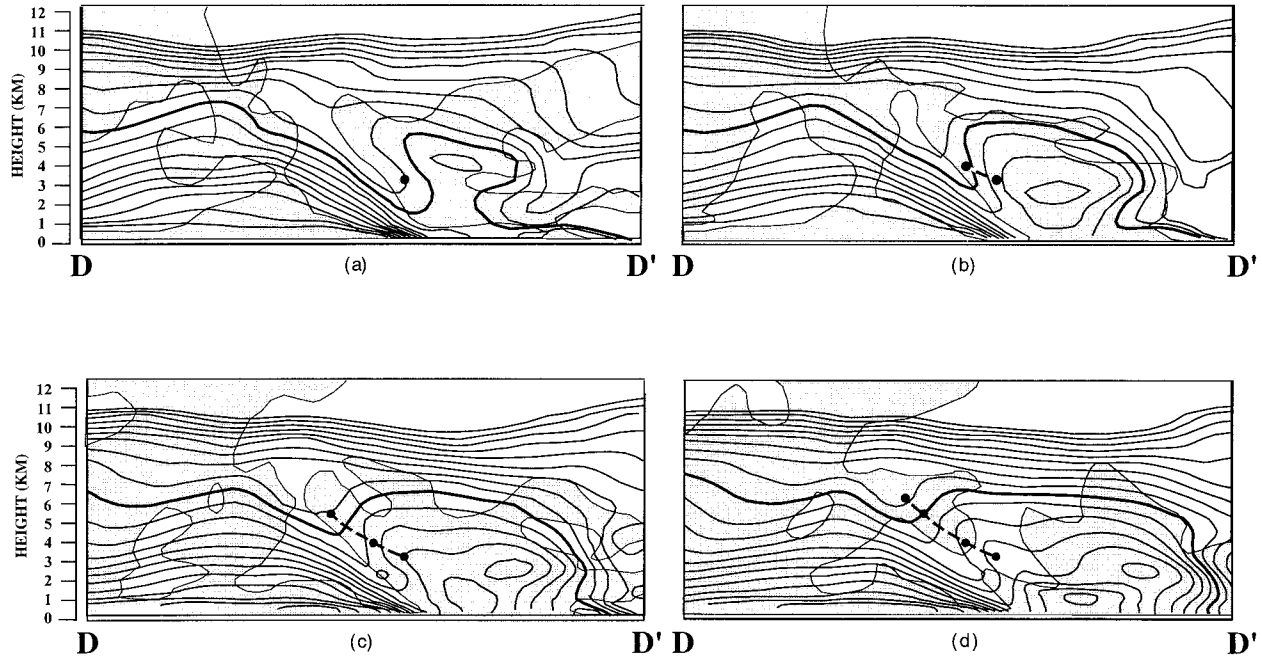

FIG. 20. (a) Vertical cross section, along line *DD′* in Fig. 19a, of equivalent potential temperature θ_e contoured every 3 K at 1600 UTC 19 January 1995. Thick solid line is θ_e = 309 K isentrope. Shaded areas are regions of horizontal cold-air advection and unshaded areas are regions of horizontal warm-air advection. The bold dot represents the 1600 UTC position of the air parcel shown in Fig. 19. (b) As for Fig. 20a except for 1900 UTC 19 January 1995. The leftmost bold dot represents the parcel position at 1900 UTC. The other dot shows the parcel's past position at 3-h intervals beginning at 1600 UTC. (c) As in Fig. 20b except for 2200 UTC 19 January 1995 and leftmost bold dot represents the parcel position at 2200 UTC. (d) As in Fig. 20b except for 0100 UTC 20 January 1995 and leftmost bold dot represents the parcel position at 0100 UTC 20 January.

acteristics makes it clear that a single cyclone event can exhibit structural elements of both the Shapiro–Keyser and Norwegian conceptual models simultaneously.

The present case was associated with the development of a cutoff cold air mass aloft (see, e.g., Fig. 14). Such cold cutoff air masses aloft must be associated with upper-level positive potential vorticity (PV) anomalies in an atmosphere in approximate thermal wind balance. Figure 21 shows the 9-km PV from the model simulation at 6-h intervals from 0000 UTC 19 January to 0600 UTC 20 January. It clearly demonstrates the merger of two originally independent features (as in Hakim et al. 1996) into one, isolated, cutoff PV feature by 0000 UTC 20 January (Fig. 21e). During this 30-h evolution, the PV anomaly was rotated cyclonically. This rotation transformed the original meridionally oriented anomaly (Fig. 21a) into a ''treble clef'' shaped anomaly most clearly identifiable in Figs. 21c–e. The treble clef upper-level PV distribution is characterized by an isolated, low-latitude high-PV feature that is connected to a high-latitude reservoir of high PV by a rather thin filament of high PV. Interestingly, a similar treble clef structure to the upper PV distribution is also present in the *cyclonic shear* simulations of Davies et al. (1991) and Thorncroft et al. (1993). Of further interest is the fact that this treble clef shape also appears in the topography of the 309-K θ_e surface, particularly above the 6-km level (see Figs. 14c–e).

Such morphological similarity between these two fields is not specific to this case but instead is a general consequence of the characteristic thermodynamic structure associated with a positive PV anomaly at tropopause level as shown by Hoskins et al. (1985) (see their Fig. 16). It was shown that the tropospheric isentropes bend upward toward the anomaly while the stratospheric isentropes bow downward toward the anomaly. Thus, regions of large PV near the tropopause sit atop relatively cold columns of air while relative minima of PV near the tropopause sit atop relatively warm columns of air. According to this description, the characteristic thermodynamic structure associated with the horizontal juxtaposition of two upper-level PV anomalies of unequal magnitude, separated by a relative minimum in PV is shown in Fig. 22. Notice that beneath the relative minimum in upper-level PV there lies an axis of highest θ (θ_e) and that this axis separates two distinct regions of tropospheric baroclinicity. This structure precisely depicts the structure of a warm occlusion and is a hydrostatic consequence of the peculiar (though not uncommon) treble clef–shaped, upper-level PV structure. Thus, we have identified a characteristic upper-level PV distribution that is a sufficient condition for asserting the

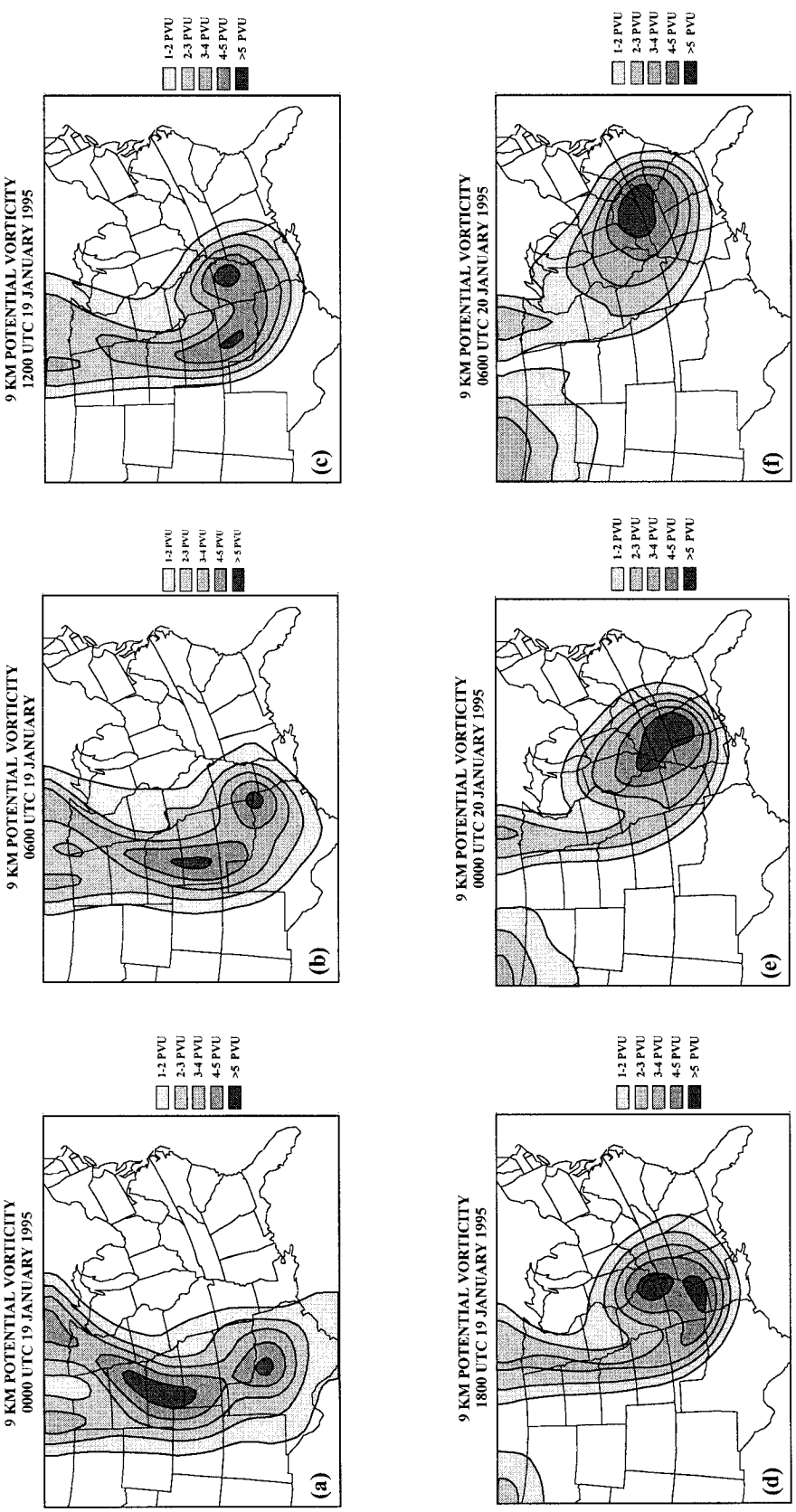

FIG. 21. (a) The 9-km potential vorticity (PV) from the UW-NMS model simulation at 0000 UTC 19 January 1995. Potential vorticity is labeled in potential vorticity units (PVU) (1 PVU $= 10^{-6}$ m^2 s^{-1} K kg^{-1}) and shaded every 1 PVU according to the legend at right. (b) As in Fig. 21a except from a 6-h forecast valid at 0600 UTC 19 January 1995. (c) As in Fig. 21a except from a 12-h forecast valid at 1200 UTC 19 January 1995. (d) As in Fig. 21a except from an 18-h forecast valid at 1800 UTC 19 January 1995. (e) As in Fig. 21a except from a 24-h forecast valid at 0000 UTC 20 January 1995. (f) As in Fig. 21a except from a 30-h forecast valid at 0600 UTC 20 January 1995.

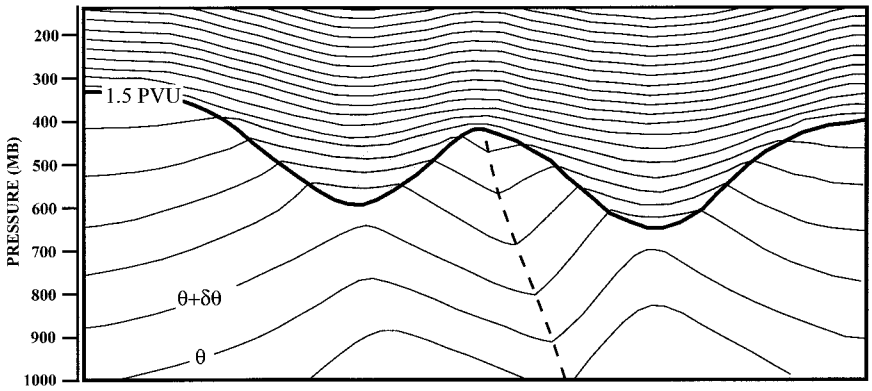

FIG. 22. Schematic representation of the thermal structure associated with horizontally juxtaposed upper-level positive PV anomalies. Thin solid lines are schematic isentropes θ. The thick solid line is the dynamic tropopause with shading indicating positive PV anomalies in the lower stratosphere. The dashed line indicates the axis of the maximum θ, which extends from the upper-tropospheric PV minimum to the surface.

presence of a cyclone with a warm-occluded structure in the underlying troposphere.

A positive upper-level PV anomaly is associated with a cyclonic circulation, the strength of which is most intense at the level of the anomaly. This circulation can be felt at lower-tropospheric levels to a degree modulated by the length scale of the anomaly as well as the ambient static stability (Hoskins et al. 1985). Despite the variations that occur in nature from case to case, it is generally true that the intensity of the cyclonic circulation associated with an upper-level PV anomaly will weaken with increasing pressure. A dynamical consequence of this fact is that thermodynamic variables at mid- and upper-tropospheric levels will generally be influenced by the circulation associated with an upper anomaly to a much greater extent than such variables near the surface. In the case of a nearly isolated vortex near the tropopause, this suggests that the cyclonic advection of high θ (θ_e) northward and westward and low θ (θ_e) southward and eastward—the exact kinematic processes necessary to form a horizontal warm-occluded structure—will proceed at a greater rate aloft than near the surface. We suggest that such a circumstance may have been responsible for the asynchronous development of the warm-occluded structure observed in this case.

7. Conclusions

From about 1800 UTC 18 January until 0600 UTC 20 January 1995, a heavy precipitation-producing cyclone affected most of the central United States. This cyclone was only modestly intense as measured by its sea level pressure minimum, which never fell below 997 hPa. Despite its lack of distinction in this regard, the cyclone was characterized by an intriguing frontal structure including a deep warm front, a cold front, and a bent-back front. This latter feature was characterized by horizontal cold-air advection near the surface and exhibited a structural resemblance to the bent-back front that has been described in association with some explosively deepening maritime cyclones (Shapiro and Keyser 1990; Neiman and Shapiro 1993). However, the evolution of this feature, which was not described here, may have been different in this case as compared to the maritime cases.

The observations of this continental bent-back front are believed to be the first such observations in the literature. The fairly weak nature of this front at the surface agrees with the theoretical work of Hines and Mechoso (1993), who considered the effects of friction on frontal structure. Frontal structures above the friction layer were not considered in that study. In the present case, the bent-back structure is most robust above the friction layer. This suggests that there may be greater similarity between the frontal structure of marine and continental cyclones than was previously thought.

The 19 January cyclone developed a warm-occluded structure during its evolution. A numerical simulation of this event using the UW-NMS was performed in order to diagnose the processes by which this occluded structure developed. It was found that the warm-occluded structure appeared first at midtropospheric levels (at 1200 UTC 19 January) and later near the surface (at 2000 UTC).

At the surface, the warm-occluded structure formed as the historical surface cold front became horizontally juxtaposed with the nearly stationary surface warm front. This is consistent with the classical model as well as with more recent model-based synoptic studies. The frontogenesis that had been sustaining the surface warm front prior to occlusion remained vigorous after occlusion. An examination of the evolution of the 309-K θ_e thermodynamic surface (located at the warm edge of the original cold- and warm-frontal zones) demonstrated that the warm-occluded structure that formed at mid-

levels resulted from a cyclonic rotation of this isosurface that led to its folding over itself in the occluded region. A representative air parcel trajectory from within the original cold-frontal zone clearly demonstrated that during the life cycle of this cyclone, cold-frontal air approached, and subsequently ascended, the warm frontal zone. Therefore, the process by which the *midlevel* warm-occluded structure developed in this cyclone was exactly the ''catch-up'' process first suggested by Bjerknes and Solberg (1922). Thus, at least some cyclones that exhibit warm-occluded structures develop those structures as a result of this occlusion mechanism.

The observed vertically asynchronous development of the warm-occluded structure was interpreted in terms of the influence of the upper-level PV anomaly associated with the cyclogenesis. It was suggested that, since, at a certain level in the troposphere, the strength of the cyclonic circulation associated with an upper-level PV anomaly is generally proportional to the distance between the anomaly and that level, that the cyclonic ''wrapping over'' of thermodynamic surfaces (such as the 309-K θ_e surface) may proceed at a faster rate at middle and upper-tropospheric levels than near the surface. As a result, warm-occluded structures may appear aloft before appearing at the surface. Such a suggestion allows for the possibility that, at a certain stage in an individual cyclone life cycle, a robust warm-occluded structure may exist at midtropospheric levels while only a fractured frontal structure exists at the surface. Since nearly all fractured frontal cyclones have been observed over the ocean [e.g., the ERICA IOP 4 storm (Neiman and Shapiro 1993)], actual observations of these storms have been made predominantly in the lower troposphere. Consequently, little information about their midtropospheric structure exists. Further examination of the deep tropospheric frontal structure of such storms is necessary in order that fair comparisons can be made between the frontal structures of oceanic and continental cyclones.

Thorncroft et al. (1993) suggested that describing the shape of the tropopause PV distribution ''may be of practical use in forecasting and also in quickly assessing the nature of synoptic events.'' Support for this suggestion is offered in the present case in which it was found that a treble clef–shaped upper-level PV anomaly characterized this cyclogenesis event. Under the dual constraints of hydrostatic and geostrophic (gradient) balance, it is suggested that such a treble clef–shaped PV anomaly *requires* a horizontal and vertical tropospheric thermal distribution that resembles a warm-occluded structure. We therefore suggest that all cyclones exhibiting this treble clef structure in the upper-level PV are likely to be characterized by warm-occluded structures in the underlying troposphere.

Acknowledgments. The author would like to thank Dr. Greg Tripoli and Peter Pokrandt for their willing and able NMS model expertise. Sebastien Korner assisted with many of the numerical model runs. Thanks also to Dr. Michael Morgan for helpful discussions concerning this work. The comments of Dr. David Schultz and an anonymous reviewer were especially helpful. This work was partially funded by the National Science Foundation under Grant ATM-9505849.

REFERENCES

Arakawa, H., 1952: The characteristic structure of the occluded frontal typhoon in the late fall other than the occlusion of wave-shaped frontal perturbations. *J. Meteor. Soc. Japan,* **30,** 211–215.

Bjerknes, J., and H. Solberg, 1922: Life cycle of cyclones and the polar front theory of atmospheric circulation. *Geofys. Publ.,* **3,** 1–18.

Castle, J. A., J. D. Locatelli, J. E. Martin, and P. V. Hobbs, 1996: Structure and evolution of winter cyclones in the central United States and their effects on the distribution of precipitation. Part IV: The evolution of a drytrough on 8–9 March 1992. *Mon. Wea. Rev.,* **124,** 1591–1595.

Chen, C., and W. R. Cotton, 1983: A one-dimensional simulation of the stratocumulus capped mixed layer. *Bound.-Layer Meteor.,* **25,** 289–321.

Cotton, W. R., G. J. Tripoli, R. M. Rauber, and E. A. Mulvihill, 1986: Numerical simulation of the effects of varying ice crystal nucleation rates and aggregation processes on orographic snowfall. *J. Climate Appl. Meteor.,* **25,** 1658–1680.

Crocker, A. M., W. L. Godson, and C. M. Penner, 1947: Frontal contour charts. *J. Meteor.,* **4,** 95–99.

Davies, H. C., C. Schar, and H. Wernli, 1991: The palette of fronts and cyclones within a baroclinic wave development. *J. Atmos. Sci.,* **48,** 1666–1689.

Douglas, C. K. M., 1929: Some aspects of surfaces of discontinuity. *Quart. J. Roy. Meteor. Soc.,* **55,** 123–151.

Emanuel, K. A., 1991: A scheme for representing cumulus convection in large-scale models. *J. Atmos. Sci.,* **48,** 2313–2335.

Flatau, P., G. J. Tripoli, J. Verlinde, and W. R. Cotton, 1989: The CSU RAMS cloud microphysical module: General theory and code documentation. Tech. Rep. 451, Dept. of Atmos. Sci., Colorado State University, 88 pp. [Available from Dept. of Atmos. Sci., CSU, Fort Collins, CO 80523.]

Funk, T. W., C. W. Hayes, M. B. Scholz, and K. A. Kostura, 1995: Vertical motion forcing mechanisms responsible for the production of a mesoscale very heavy snow band. Preprints, *14th Conf. on Weather Analysis and Forecasting,* Dallas, TX, Amer. Meteor. Soc., 176–181.

Galloway, J. L., 1958: The three-front model: Its philosophy, nature, construction and use. *Weather,* **13,** 3–10.

——, 1960: The three-front model, the developing depression and the occluding process. *Weather,* **15,** 293–301.

Godson, W. L., 1951: Synoptic properties of frontal surfaces. *Quart. J. Roy. Meteor. Soc.,* **77,** 633–653.

Hakim, G. J., L. F. Bosart, and D. Keyser, 1995: The Ohio Valley wave-merger cyclogenesis event of 25–26 January 1978. Part I: Multiscale case study. *Mon. Wea. Rev.,* **123,** 2663–2692.

——, D. Keyser, and L. F. Bosart, 1996: The Ohio Valley wave-merger cyclogenesis event of 25–26 January 1978. Part II: Diagnosis using quasigeostrophic potential vorticity inversion. *Mon. Wea. Rev.,* **124,** 2176–2205.

Hines, K. M., and C. R. Mechoso, 1993: Influence of surface drag on the evolution of fronts. *Mon. Wea. Rev.,* **121,** 1152–1175.

Hobbs, P. V., J. D. Locatelli, and J. E. Martin, 1990: Cold fronts aloft and the forecasting of precipitation and severe weather east of the Rocky Mountains. *Wea. Forecasting,* **5,** 613–626.

——, ——, and ——, 1996: A new conceptual model for cyclones generated in the lee of the Rocky Mountains. *Bull. Amer. Meteor. Soc.,* **77,** 1169–1178.

Hoskins, B. J., 1990: Theory of extratropical cyclones. *Extratropical Cyclones: The Erik Palmén Memorial Volume,* C. W. Newton and E. O. Halopainen, Eds., Amer. Meteor. Soc., 63–80.

——, M. E. McIntyre, and A. W. Robertson, 1985: On the use and significance of isentropic potential vorticity maps. *Quart. J. Roy. Meteor. Soc.,* **111,** 877–946.

Keshishian, L. G., L. F. Bosart, and W. E. Bracken, 1994: Inverted troughs and cyclogenesis over interior North America: A limited regional climatology and case studies. *Mon. Wea. Rev.*, **122,** 565–607.

Keyser, D., and M. A. Shapiro, 1986: A review of the structure and dynamics of upper-level frontal zones. *Mon. Wea. Rev.*, **114,** 452–499.

Kuo, Y.-H., and R. J. Reed, 1988: Numerical simulation of an explosively deepening cyclone in the eastern Pacific. *Mon. Wea. Rev.*, **116,** 2081–2105.

——, ——, and S. Low-Nam, 1992: Thermal structure and airflow in a model simulation of an occluded marine cyclone. *Mon. Wea. Rev.*, **120,** 2280–2297.

Locatelli, J. D., J. M. Sienkiewicz, and P. V. Hobbs, 1989: Organization and structure of clouds and precipitation on the mid-Atlantic coast of the United States. Part I: Synoptic evolution of a frontal system from the Rockies to the Atlantic coast. *J. Atmos. Sci.,* **46,** 1337–1348.

——, J. E. Martin, J. A. Castle, and P. V. Hobbs, 1995: Structure and evolution of winter cyclones in the central United States and their effects on the distribution of precipitation. Part III: The development of a squall line associated with weak cold frontogenesis aloft. *Mon. Wea. Rev.,* **123,** 2641–2662.

Martin, J. E., 1998: The structure and evolution of a continental winter cyclone. Part II: Frontal forcing of an extreme snow event. *Mon. Wea. Rev.,* **126,** 329–348.

——, J. D. Locatelli, and P. V. Hobbs, 1990: Organization and structure of clouds and precipitation on the mid-Atlantic coast of the United States. Part III: The evolution of a middle tropospheric cold front. *Mon. Wea. Rev.,* **118,** 195–217.

——, ——, and ——, 1992: Organization and structure of clouds and precipitation on the mid-Atlantic coast of the United States. Part V: The role of an upper-level front in the generation of a rainband. *J. Atmos. Sci.,* **49,** 1293–1303.

——, ——, ——, P.-Y. Wang, and J. A. Castle, 1995: Structure and evolution of winter cyclones in the central United States and their effects on the distribution of precipitation. Part I: A synoptic-scale rainband associated with a dryline and a lee trough. *Mon. Wea. Rev.,* **123,** 241–264.

Marwitz, J., and J. Toth, 1993: A case study of heavy snowfall in Oklahoma. *Mon Wea. Rev.,* **121,** 648–660.

Mass, C. F., and D. M. Schultz, 1993: The structure and evolution of a simulated midlatitude cyclone over land. *Mon. Wea. Rev.,* **121,** 105–117.

Moore, J. T., and P. D. Blakely, 1988: The role of frontogenetical forcing and conditional symmetric instability in the Midwest snowstorm of 30–31 January 1982. *Mon. Wea. Rev.,* **116,** 2155–2171.

Nieman, P. J., and M. A. Shapiro, 1993: The life cycle of an extratropical marine cyclone. Part I: Frontal-cyclone evolution and thermodynamic air–sea interaction. *Mon. Wea. Rev.,* **121,** 2153–2176.

Palmén, E., 1951: The aerology of extratropical disturbances. *Compendium of Meteorology,* T. F. Malone, Ed., Amer. Meteor. Soc., 599–620.

Penner, C. M., 1955: A three-front model for synoptic analyses. *Quart. J. Roy. Meteor. Soc.,* **81,** 89–91.

Pokrandt, P. J., G. J. Tripoli, and D. D. Houghton, 1996: Processes leading to the formation of the mesoscale waves in the Midwest cyclone of 15 December 1987. *Mon. Wea. Rev.,* **124,** 2726–2752.

Powers, J. G., and R. J. Reed, 1993: Numerical simulation of the large-amplitude mesoscale gravity-wave event of 15 December 1987 in the central United States. *Mon. Wea. Rev.,* **121,** 2285–2308.

Rauber, R. M., M. K. Ramamurthy, and A. Tokay, 1994: Synoptic and mesoscale structure of a severe freezing rain event: The St. Valentine's Day ice storm. *Wea. Forecasting,* **9,** 183–208.

Sadourny, R., 1975: The dynamics of finite-difference models of the shallow water equations. *J. Atmos. Sci.,* **32,** 680–689.

Schneider, R. S., 1990: Large amplitude mesoscale wave disturbances within the intense Midwest extratropical cyclone of 15 December 1987. *Wea. Forecasting,* **5,** 533–558.

Schultz, D. M., and C. F. Mass, 1993: The occlusion process in a midlatitude cyclone over land. *Mon. Wea. Rev.,* **121,** 918–940.

Shapiro, M. A., 1981: Frontogenesis and geostrophically forced secondary circulations in the vicinity of jet stream–frontal zone systems. *J. Atmos. Sci.,* **38,** 954–973.

——, and D. Keyser, 1990: Fronts, jet streams and the tropopause. *Extratropical Cyclones: The Erik Palmén Memorial Volume,* C. W. Newton and E. Holopainen, Eds., Amer. Meteor. Soc., 167–191.

——, and E. Donall Grell, 1994: In search of synoptic/dynamic conceptualizations of the life cycles of fronts, jet streams, and the tropopause. Vol. 1, *The Life Cycles of Extratropical Cyclones,* S. Gronas and M. A. Shapiro, Eds., Aase Grafiske A/S, Stavanger, 163–181.

Shea, T. J., and R. W. Przybylinski, 1993: Assessing vertical motion fields in a winter storm using PCGRIDDS. Preprints, *13th Conf. on Weather Analysis and Forecasting,* Vienna, VA, Amer. Meteor. Soc., 10–14.

——, and ——, 1995: Forecasting the northern extent of significant snowfall in a major winter storm: An operational forecasting problem. Preprints, *14th Conf. on Weather Analysis and Forecasting,* Dallas, TX, Amer. Meteor. Soc., 280–285.

Thorncroft, C. D., B. J. Hoskins, and M. E. McIntyre, 1993: Two paradigms of baroclinic-wave life-cycle behaviour. *Quart. J. Roy. Meteor. Soc.,* **119,** 17–55.

Tremback, C. J., and R. Kessler, 1985: A surface temperature and moisture parameterization for use in mesoscale numerical models. Preprints, *Seventh Conf. on Numerical Weather Prediction,* Montreal, PQ, Canada, Amer. Meteor. Soc., 355–358.

——, J. Powell, W. R. Cotton, and R. A. Pielke, 1987: The forward-in-time upstream advection scheme: Extension to higher orders. *Mon. Wea. Rev.,* **115,** 540–555.

Tripoli, G. J., 1992a: An explicit three-dimensional nonhydrostatic numerical simulation of a tropical cyclone. *Meteor. Atmos. Phys.,* **49,** 229–254.

——, 1992b: A nonhydrostatic numerical model designed to simulate scale interaction. *Mon. Wea. Rev.,* **120,** 1342–1359.

Uccellini, L. W., and S. E. Koch, 1987: The synoptic setting and possible energy sources for mesoscale wave disturbances. *Mon. Wea. Rev.,* **115,** 721–729.

Wallace, J. M., and P. V. Hobbs, 1977: *Atmospheric Science: An Introductory Survey.* Academic Press, 467 pp.

Wang, P.-Y., J. E. Martin, J. D. Locatelli, and P. V. Hobbs, 1995: Structure and evolution of winter cyclones in the central United States and their effects on the distribution of precipitation. Part II: Arctic fronts. *Mon. Wea. Rev.,* **123,** 1328–1344.